bblt **Version 7.0 User's Manual**

Adam Drozdowski, Charles Hannah, Ted Tedford

Ocean Sciences Division
Maritimes Region
Fisheries and Oceans Canada

Bedford Institute of Oceanography
P.O. Box 1006
Dartmouth, Nova Scotia
Canada B2Y 4A2

2004

Canadian Technical Report of Hydrography and Ocean Sciences 240

Fisheries and Oceans Canada | Pêches et Océans Canada

Canada

Canadian Technical Report of Hydrography and Ocean Sciences

Technical reports contain scientific and technical information of a type that represents a contribution to existing knowledge but which is not normally found in the primary literature. The subject matter is generally related to programs and interests of the Oceans and Science sectors of Fisheries and Oceans Canada.

Technical reports may be cited as full publications. The correct citation appears above the abstract of each report. Each report is abstracted in the data base *Aquatic Sciences and Fisheries Abstracts*.

Technical reports are produced regionally but are numbered nationally. Requests for individual reports will be filled by the issuing establishment listed on the front cover and title page. Out-of-stock reports will be supplied for a fee by commercial agents.

Regional and headquarters establishments of Ocean Science and Surveys ceased publication of their various report series as of December 1981. A complete listing of these publications and the last number issued under each title are published in the *Canadian Journal of Fisheries and Aquatic Sciences*, Volume 38: Index to Publications 1981. The current series began with Report Number 1 in January 1982.

Rapport technique canadien sur l'hydrographie et les sciences océaniques

Les rapports techniques contiennent des renseignements scientifiques et techniques qui constituent une contribution aux connaissances actuelles mais que l'on ne trouve pas normalement dans les revues scientifiques. Le sujet est généralement rattaché aux programmes et intérêts des secteurs des Océans et des Sciences de Pêches et Océans Canada.

Les rapports techniques peuvent être cités comme des publications à part entière. Le titre exact figure au-dessus du résumé de chaque rapport. Les rapports techniques sont résumés dans la base de données *Résumés des sciences aquatiques et halieutiques*.

Les rapports techniques sont produits à l'échelon régional, mais numérotés à l'échelon national. Les demandes de rapports seront satisfaites par l'établissement auteur dont le nom figure sur la couverture et la page de titre. Les rapports épuisés seront fournis contre rétribution par des agents commerciaux.

Les établissements de l'ancien secteur des Sciences et Levés océaniques dans les régions et à l'administration centrale ont cessé de publier leurs diverses séries de rapports en décembre 1981. Vous trouverez dans l'index des publications du volume 38 du *Journal canadien des sciences halieutiques et aquatiques*, la liste de ces publications ainsi que le dernier numéro paru dans chaque catégorie. La nouvelle série a commencé avec la publication du rapport numéro 1 en janvier 1982.

104-07730/

Canadian Technical Report of
Hydrography and Ocean Sciences 240

2004

bblt Version 7.0 User's Manual

by

Adam Drozdowski, Charles Hannah, Ted Tedford

Ocean Sciences Division
Maritimes Region
Fisheries and Oceans Canada

Bedford Institute of Oceanography
P.O. Box 1006
Dartmouth, N.S.
Canada B2Y 4A2

©Her Majesty the Queen in Right of Canada 2004
Cat. No. Fs 97-18/240E ISSN 0711-6764

Correct citation for this publication:

Drozdowski, A., Hannah, C. G. and Tedford, T. 2004. `bblt` Version 7.0 User's Manual. Can. Tech. Rep. Hydrogr. Ocean Sci. 240: vi + 69 pp.

Table of Contents

List of Figures v

List of Tables v

Abstract/Résumé vi

1 Introduction 1

2 The features of `bblt` Version 7.0 3

3 The Theory behind `bblt` 4
- 3.1 Transport and Shear Dispersion . . . 4
- 3.2 Bottom Stress . . . 6
- 3.3 Settling Velocity . . . 7
- 3.4 Modified Rouse Profile . . . 8
- 3.5 The Particle Model . . . 11
- 3.6 Vertical Shuffling . . . 13
- 3.7 Vertical Shear . . . 14
- 3.8 Biological Impact Module . . . 15
- 3.9 Model Output and Derived Quantities . . . 16

4 Software Overview 18

5 Input Parameters 24
- 5.1 General Description . . . 24
- 5.2 Parameter Input File . . . 28

6 Sample `bblt` run 33
- 6.1 Input . . . 33
- 6.2 Output . . . 33
  - 6.2.1 Sediment parameters file . . . 36
  - 6.2.2 Velocity file . . . 38
  - 6.2.3 Statistics file . . . 38
  - 6.2.4 Packet positions file . . . 39
  - 6.2.5 Concentration time series file . . . 40
  - 6.2.6 Concentration map file . . . 41
  - 6.2.7 Biological impacts file . . . 42
  - 6.2.8 Biological impacts map file . . . 42

7 Final Comments 43

A List of Symbols 47

B Logarithmic Sublayer **49**

C SEDTRANS96 **51**

D Validation Through Numerical Experiments **53**
D.1 Steady and Rotary Flow Theory 53
D.2 Numerical Experiments 55

E Sample Input File **60**

F Sample Input Time Series **63**
F.1 Friction Velocity Time Series 63
F.2 Discharge Time Series 63
F.3 Velocity Time Series 64

G Sample Auxiliary Files **65**
G.1 Log-layer File 65
G.2 Height File 66

H Sample Outputs **66**
H.1 Sediment Parameters File 66
H.2 Statistics File 67
H.3 Concentration File 68
H.4 Biological Impacts File 68

List of Figures

1 Schematic flow chart for the bblt models 2
2 Shear dispersion 5
3 Shear dispersion of a vertical line of particles 6
4 The stress-dependent settling velocity 8
5 1-layer and 2-layer formulation 10
6 Schematic of shearing and shuffling packets 14
7 Schematic time line 26
8 The vertical coordinate scheme 27
9 GUI input file cross-reference 34
10 GUI input and output windows 35
11 Velocity file input window 36
12 GUI plots of input time series. 37
13 Sediment plot selection and Rouse plot 38
14 Statistics plot selection and mean height 39
15 Concentration output plot selection window 40
16 A snapshot of the concentration map. 41
17 A sample biological impacts map. 42
18 Schematic of inputs, outputs and processes. 52
19 Diffusivity as a function of t_m for steady and rotary flow. 57
20 Packet variance as a function of time for rotary flow 58
21 The diffusivity as a function of the strength of the mixing 61

List of Tables

1 Outline of the algorithm for bblt v7.0. 19
2 List of bblt v7.0 input parameter symbols 25
3 The four Rouse numbers calculated by bblt v7.0 36
4 Parameter values for numerical experiments 56

Abstract

Drozdowski, A., Hannah, C. G. and Tedford, T. 2004. `bblt` Version 7.0 User's Manual. Can. Tech. Rep. Hydrogr. Ocean Sci. 240: vi + 69 pp.

The fate and potential environmental impacts of discharged drilling muds are ongoing issues for offshore petroleum operators, regulators, government agencies and environmentalists. The benthic boundary layer transport model, `bblt`, was developed to predict the transport and dispersion of suspended particulate drill waste in the benthic boundary layer. The latest version of `bblt` (Version 7.0) includes a graphical user interface (GUI) with integrated graphical output. The GUI is written in Java to enhance portability. Recent technical developments include a stress dependent settling velocity, explicit representation of the wave-current boundary layer, and a biological impacts module. As with previous releases, `bblt v7.0` assumes a spatially homogeneous environment; horizontal variations in water depth, currents and bottom stress are ignored. The software can be downloaded from the web and installed on computers running either Linux or MS-Windows. The installation includes the source code for both the core `bblt` code and the GUI.

Résumé

Drozdowski, A., Hannah, C. G. and Tedford, T. 2004. `bblt` Version 7.0 User's Manual. Can. Tech. Rep. Hydrogr. Ocean Sci. 240: vi + 69 pp.

L'avenir des décharges de boues de forage et leur influence potentielle sur l'environnement constituent un problème récurrent pour les opérateurs de pétrole en mer, les régulateurs, les organismes gouvernementaux et les écologistes. Le modèle benthique de transport de couche limite, `bblt`, a été développé pour prévoir le transport et la dispersion des particules en suspension issues des pertes de forage dans la couche limite benthique. La dernière version de `bblt` (version 7.0) inclut une interface utilisateur graphique (GUI) avec graphiques intégrés. Le GUI est écrit en Java pour améliorer la portabilité. Les développements techniques récents incluent en sortie de logiciel une vitesse de chûte dépendante de la contrainte, une représentation explicite de la couche limite vague-courant, et un module d'impacts biologiques. Comme avec les distributions précédentes, `bblt v7.0` suppose un environnement homogène dans l'espace: les variations horizontales de la profondeur de l'eau, des courants et de la contrainte du fond marin sont ignorées. Le logiciel peut être téléchargé à partir du web et être installé sur des ordinateurs d'environment Linux ou MS-Windows. L'installation inclut le code source pour, à la fois, le `bblt` et le GUI.

1 Introduction

The fate and potential environmental impacts of discharged drilling muds are ongoing issues for offshore petroleum operators, regulators, government agencies and environmentalists, particularly with multiple development and exploration sites in close proximity to each other on Sable Bank and the northeast Grand Bank (e.g. Gordon et al., 2000).

The benthic boundary layer transport model, `bblt`, was developed to predict the transport and dispersion of suspended particulate drill waste in the benthic boundary layer. The primary components of water based mud are barite ($BaSO_4$; a weighting agent) and bentonite (a clay mineral). Laboratory studies have shown sublethal effects on scallops from both materials (Cranford and Gordon, 1992; Cranford et al., 1999). The focus has been on the near-bottom concentrations because both flocculated drill mud fines (bentonite) and single grains of barite particles can have settling velocities which allow them to be concentrated near the seafloor (Muschenheim et al., 1995; Muschenheim and Milligan, 1996). The model combines estimates of the current profile, the bottom stress, the sediment concentration profile, and the discharge scenario to generate estimates of drift, dispersion, and concentration (Figure 1).

Here we report on the latest technical developments in `bblt`, version 7.0, which has several technical improvements over the previous release `bblt v3.1` (Tedford et al., 2001) including a stress dependent settling velocity (Tedford et al., 2003), explicit representation of the wave-current boundary layer (Li and Amos, 2001), a biological impacts module (Cranford et al., 2003), and two new vertical shuffling algorithms. An important new feature is a graphical user interface (GUI) with integrated graphical output. The software can be downloaded from the web and installed on computers running either Linux or MS-Windows. The installation includes the source code for both the core `bblt` code and the GUI.

As with previous releases, `bblt v7.0` assumes a spatially homogeneous environment; horizontal variations in water depth, currents and bottom stress are ignored (Hannah et al., 1995, 1996). This simplification results in a major reduction in computational demand, while retaining the effects of vertical and temporal variations in the current which are generally the primary factors in short-term dispersion and transport at local positions.

The developments of `bblt` have been documented by Hannah et al. (1995, 1996, 1998), Loder et al. (1998) and Xu et al. (2000). The application of `bblt` as one component of an impacts zone assessment model for Georges Bank is documented by Loder et al. (1998), Gordon et al. (2000), and Boudreau et al. (1999). This line of development culminated in the release of `bblt v3.1` (Tedford et al., 2001). Recent applications and descriptions of the technical developments that are now part of `bblt v7.0` can be found in Tedford et al. (2003) and Hannah et al. (2003). Hannah et al. (1995) remains a useful description of the basic processes represented in `bblt`.

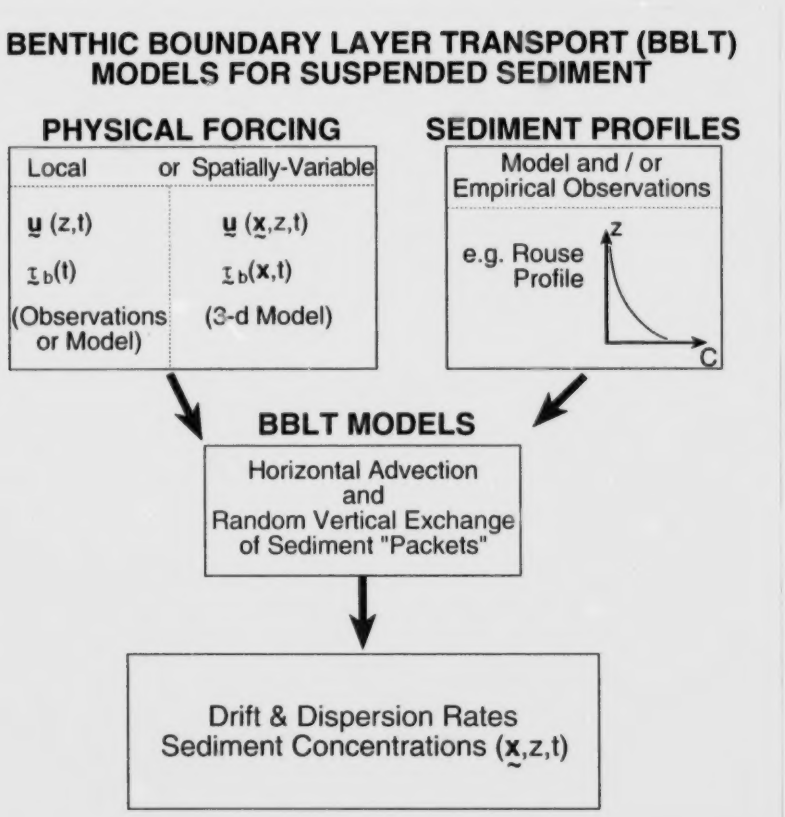

Figure 1: Schematic flow chart for the `bblt` models. Quantitative information on currents, bottom stress and the vertical structure of suspended sediment is used in the models to estimate sediment drift and dispersion rates. Only local `bblt` is discussed in this report. For a discussion of the spatially variable `bblt` see Xu et al. (2000).

This report is a complete user's guide to `bblt v7.0` and includes an overview of the features available with this release version (Section 2); a discussion of the basic concepts and theory pertinent to `bblt v7.0` (Section 3); an overview of the software (Section 4); a description of the required input parameters and forcing functions (Section 5); and a sample run of `bblt v7.0` with a demonstration of the GUI (Section 6). Appendix A contains a list of symbols used in the text. Appendix B gives a description of the logarithmic bottom boundary layer used by `bblt v7.0`, while Appendix C explains SEDTRANS96, a code that is useful for generating time series of bottom stress that include wave-current interactions. Appendix D contains an account of numerical experiments that validate some of basic concepts of `bblt`. Appendices E through to H, contain samples of `bblt v7.0` input, auxiliary and output files.

2 The features of bblt Version 7.0

Graphical User Interface A graphical user interface (GUI) was created for `bblt v7.0`. Data can be loaded from input files or entered manually. Changes can then be made and saved, and `bblt` run directly from the GUI. Selected inputs and outputs can also be plotted. The GUI is written in Java to enhance portability and graphics implemented using an open source Java class library. The GUI is discussed further in Sections 4, 5.2 and 6.

Wave-current Boundary Layer A wave-current boundary layer was introduced following Grant and Madsen (1986) and Li and Amos (2001). The resulting concentration profile has 2 layers: a wave-current boundary layer forced by the stress due to the combined effect of waves and currents and above that a layer forced by the stress due to the currents only. The original single layer formulation is also available. Refer to Section 3.4 for a discussion.

Biological Impacts Module `bblt` now contains a biological impacts module based on a growth-days lost formulation determined from laboratory experiments on scallops (Cranford et al., 2003). User specified parameters are the no-effect and no-growth concentrations (Section 3.8).

Discharge Scenarios `bblt v7.0` can handle 3 types of sediment discharge scenarios: Bulk dump, simple continuous release and arbitrary time series release. In the bulk release all the sediment is discharged at the start of the simulation. In continuous release, the discharge is spread evenly over a specified time interval. Most generally, a discharge time series can be used.

Settling Velocity and Floc Breakup The settling velocity of the sediment can be fixed or bottom-stress dependent. In the stress dependent case, the sediment particles (called packets in `bblt`, Section 3.5), exist in one of three settling velocity states as determined by the critical breakup stress (Section 3.3).

Current Meters `bblt` requires time series of current velocity at one horizontal location and arbitrary vertical positions (Section 5.1). The time series can come from field observations or numerical models. Linear interpolation is used between vertical positions. The phrase 'current meter' is used as shorthand for 'time series of velocity' in this report.

Bottom Stress The bottom stress can be specified by a time series or computed from the bottom current meter using a polynomial stress law. With the time series formulation, the user can invoke the current-wave boundary layer or restrict `bblt` to the 1-layer mode (Section 3.2).

Logarithmic Bottom Layer. The vertical structure of the velocity below the bottom current meter is computed using a log-layer formulation This is a reasonable approximation for use with currents within a few metres of the seafloor, but a crude one for currents at greater distances above the seafloor. The formulation also allows for a linear vertical structure. Details regarding the implementation of the logarithmic layer are provided in Appendix B.

Maximum Sediment Profile Height. The maximum height (h_{max}) of the concentration profile must be specified. This feature is particularly important in areas where stratification limits the height of the bottom mixed layer beyond that implied by the unrestricted Rouse profile.

Vertical Mixing Vertical mixing occurs through shuffling of the vertical positions of the packets. `bblt v7.0` offers 4 shuffling algorithms: no mixing, randomly selected pair swaps (original algorithm), systematically selected pair swaps or randomly selected vertical position. This topic is discussed in detail in Section 3.6 and Appendix D.2.

Statistical Calculations The code produces time series of statistical information describing the sediment distribution at different times. This information consists of the 3D center of mass, variance along the major and minor axis, orientation of major axis, 2D and near-bottom 3D concentration at center of mass (Section 3.9).

Concentration Calculation `bblt v7.0` can compute time series of concentration at user-specified locations and on a regular grid. The calculation involves counting packets in a prescribed area and inferring the volumetric concentration at the specified vertical location (Section 3.9).

3 The Theory behind `bblt`

3.1 Transport and Shear Dispersion

The conceptual model of suspended sediment transport that forms the foundation of `bblt` is illustrated in Figure 2. Consider an initial distribution of sediment (time 1). The currents and bottom stress increase and suspend additional sediment (time 2). The distribution of suspended sediment is stretched in the horizontal by vertical shear in the currents and redistributed vertically by vertical mixing (time 3). Finally, the currents relax and sediment settles back to the bottom, with a broader distribution and new horizontal center of mass (time 4).

The primary dispersion mechanism in the model is shear dispersion, in our case, horizontal dispersion due to the interaction of vertical mixing and vertical shear. Figure 3 illustrates the idea that in a purely periodic flow (here, rectilinear), an initial line of

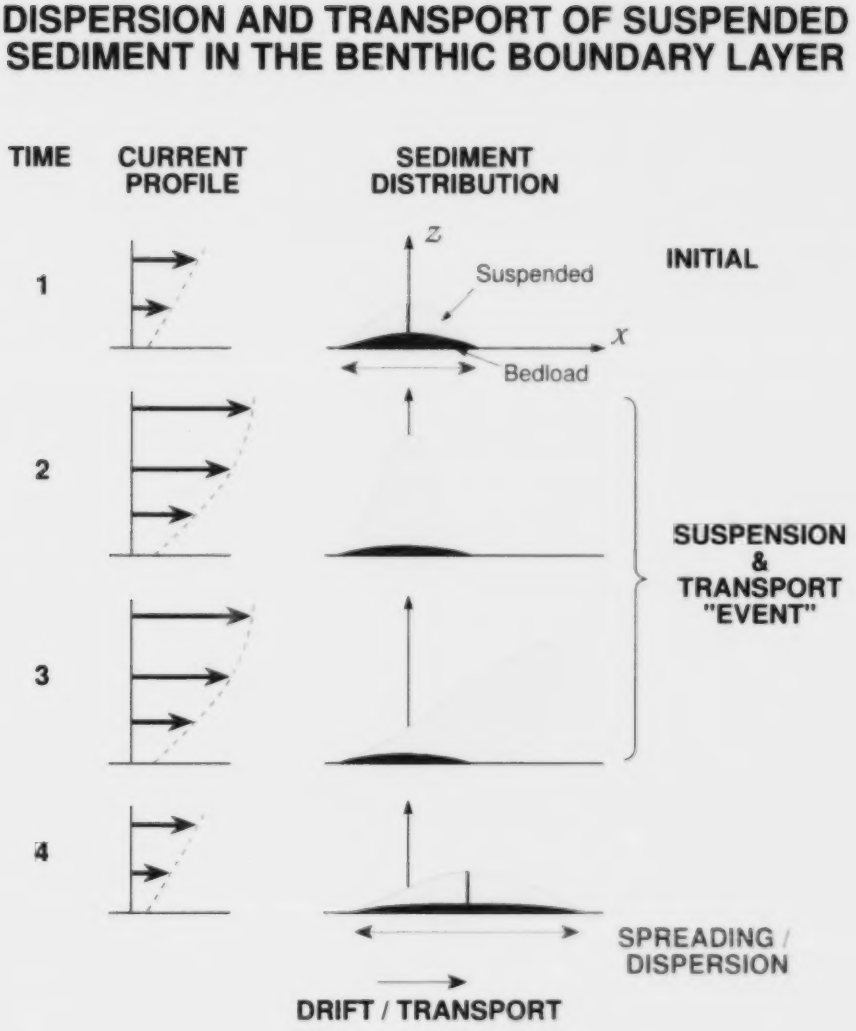

Figure 2: Schematic illustrating how sediment suspension and vertical shear in horizontal currents in the benthic boundary layer lead to horizontal drift and shear dispersion.

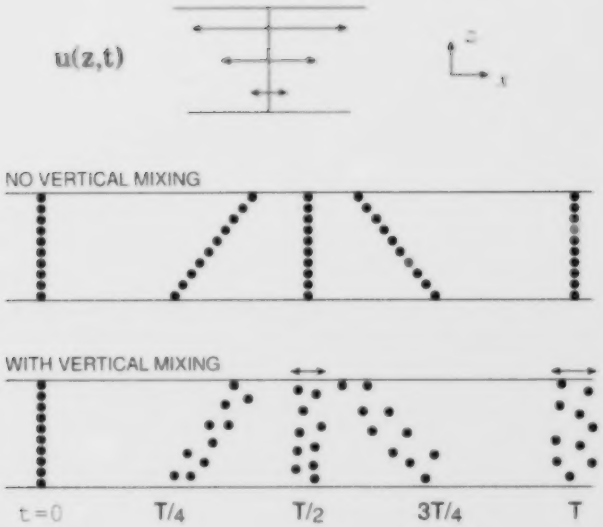

Figure 3: Schematic of shear dispersion of a vertical line of particles in a horizontal tidal current with vertical shear. Vertical mixing is required for horizontal dispersion over a tidal period. The case shown (a tilt in each direction during each tidal period) assumes peak currents at $t = 0$ ($u = \cos \omega t$).

particles can be smeared out due to the interaction of vertical mixing and vertical shear (Fischer et al., 1979). In the absence of vertical mixing, the vertical line of particles is tilted back and forth over the tidal period but there is no net dispersion. On the other hand, in the presence of vertical mixing, particles are displaced vertically from the tilted line, resulting in horizontal dispersion during each periodic tilting.

3.2 Bottom Stress

The terms bottom stress and friction velocity are often used interchangeably. In this report, the former typically refers to the physical quantity and the latter to the specific choice of units for `bblt` input. The friction velocity $u_* = \sqrt{\tau_b/\rho}$ where τ_b is the magnitude of the bottom stress and ρ is the density of sea water.

In `bblt`, u_* is either imported as a time series or calculated from the near-bottom currents. When a time series of friction velocity is provided, either the 1-layer or 2-layer boundary formulation can be invoked. If the user can provide the time series of stress due to the combined effect of waves and currents (u_{*cw}), the stress due to the currents (u_{*c}) and the wave boundary layer height (δ), then the 2-layer formulation for the concentration profile can be used. Otherwise the 1-layer formulation is used (Section 3.4 and 5.2).

If a time series of friction velocity is not provided, a polynomial stress law is used

$$u_*^2 = \sum_{i=0}^{I} a_i |\mathbf{u}_b|^i \tag{1}$$

where $|\mathbf{u}_b|$ is the magnitude of the observed near-bottom current and the a_i are the I user-specified bottom friction parameters.

Recent applications of `bblt`, such as Tedford et al. (2003) and Hannah et al. (2003), used SEDTRANS96 (Li and Amos, 2001) to compute the bottom stress based on the combined effect of the observed currents and waves. Because of its continued importance to `bblt`, SEDTRANS96 is described in Appendix C.

3.3 Settling Velocity

`bblt v7.0` offers two settling velocity scenarios: fixed and stress dependent. The fixed case uses a single number to describe the settling usually either fast (typically 0.5 $\mathrm{cm\,s^{-1}}$) which will give large near-bottom concentrations under most conditions or slow (typically 0.1 $\mathrm{cm\,s^{-1}}$) which will give substantially smaller near-bottom concentrations.

For the stress dependent settling velocity case (Figure 4), a simple flocculation routine was incorporated into `bblt v7.0`. Flocs are initially assigned a fast settling velocity, w_0 (typically 0.5 $\mathrm{cm\,s^{-1}}$), to match the large flocs expected to occur in the early stages (high concentration) of the discharge plume (Milligan and Hill, 1998). This settling velocity will give large near-bottom concentrations under most conditions. The settling velocity remains at this value until the friction velocity (u_*) exceeds the critical value u_*^c when the flocs breakup into their individual components which have a very slow settling velocity, w_2 (typically 0.01 $\mathrm{cm\,s^{-1}}$). This leads to a nearly uniform vertical distribution. When u_* once again falls below u_*^c, the material becomes incorporated into the background of marine flocs with settling velocity, w_1 (typically 0.1 $\mathrm{cm\,s^{-1}}$). Thereafter the settling velocity is w_1 when $u_* \leq u_*^c$ and w_2 when $u_* > u_*^c$.

The typical value used for w_0 is the modal value for flocs observed by Milligan and Hill (1998) in their flocculation experiments with water based muds. The typical value of w_1 is based on the settling velocity observed for naturally occurring marine flocs (Hill et al., 1998, 2000). A reasonable value for the critical stress is $u_*^c = 1.0$ $\mathrm{cm\,s^{-1}}$ (equivalent to 0.1 Pa, Hill et al., 2001)). This approach is most applicable to the bulk discharge of water-based mud, when the large discharge volumes can create a high concentration plume where rapid flocculation can occur.

The settling velocity scenario described above is suitable for very fine components of drill mud, such as bentonite, which is likely to be incorporated into the background floc population. A material such as barite, which is more granular and whose single grain settling velocity is of the same order as the background floc population, is better modelled with $w_1 = w_2$ with w_1 equal to the modal value of the individual grain settling velocity.

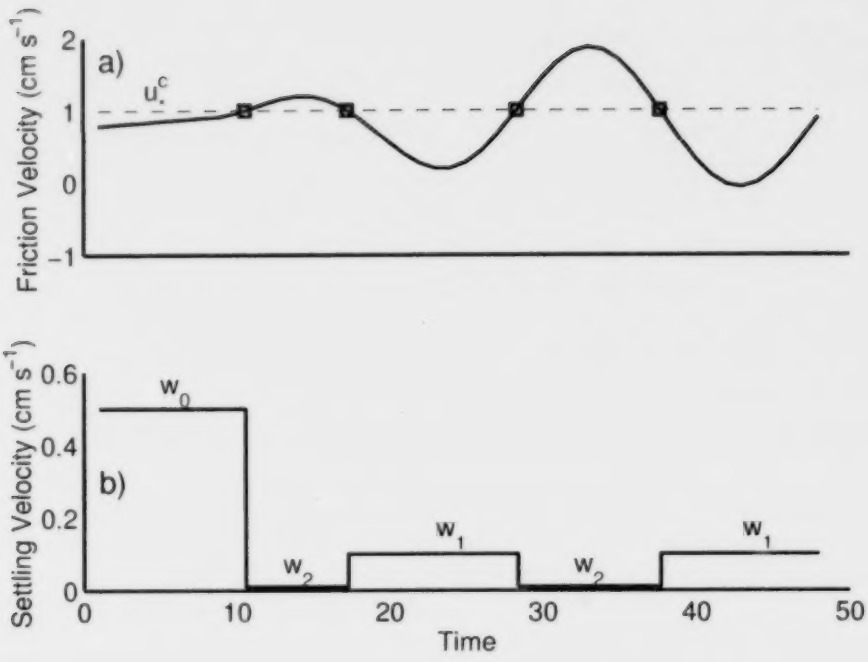

Figure 4: An illustration of the stress-dependent settling velocity: a) simplified time series of friction velocity; b) time series of the settling velocity. The square markers in a) show when breakup/flocculation occurs.

The settling velocity model proposed here assumes that the flocculation is instantaneous. While not instantaneous, Hill et al. (2001) estimate a flocculation time scale of 900 seconds, which is shorter than the hourly time scale of the currents observations.

3.4 Modified Rouse Profile

In the formulation of `bblt`, there was an implicit assumption that the sediment particles have a significant settling velocity and therefore, for a bottom source of sediment, the concentration profile is maximum near the bottom and decreases monotonically towards the surface. This assumption is made explicit by our use of a modified Rouse concentration profile.

The Rouse profile (Rouse 1937; Dyer 1986; van Rijn 1993) is a solution to the 1-dimensional steady state advective-diffusion equation:

$$c(z)\, w_s + \epsilon(z)\, \frac{\mathrm{d}c(z)}{\mathrm{d}z} = 0, \tag{2}$$

where $c(z)$ is the time averaged sediment concentration at height z above the sea floor, w_s is the particle settling velocity, and $\epsilon(z)$ is the mixing coefficient at height z above

the sea floor. The solution has the form

$$\frac{c}{c_a} = \left(\frac{h-z}{z} \frac{a}{h-a} \right)^p \tag{3}$$

where c_a is the reference concentration at the reference height $z = a$ above the sea floor, and h is the water depth. The reference height is taken as the lower boundary of the suspended sediment profile. Particle motion below a is assumed to be negligible and is ignored in `bblt`. The Rouse number is $p = w_s/(\kappa u_*)$ with the von Karman constant $\kappa = 0.4$ and friction velocity u_*.

Equation (3) has a history of reasonable agreement with flume experiments (van Rijn 1993, Chapter 7). One significant drawback of (3) is that it enforces zero concentration at the surface: $c(h) = 0$. The vertical concentration profile used by `bblt` is the modified Rouse profile

$$c(z) = c_a(a/z)^p \tag{4}$$

which is an approximation to (3) in the limit $z/h \ll 1$ and $a/h \ll 1$. The latter is a good approximation, the former is questionable for small values of p. However (4) is easy to manipulate mathematically and is quite useful for proof of principal. The differences between (3) and (4) are confined to the upper water column where (3) is forced to zero and (4) decays slowly.

Notice that, using (4),

$$\int_a^\infty c(z)\mathrm{d}z$$

does not converge for $p \leq 1$. This is an important point and serves as a reminder that (4) is intended as a near-bottom relation. An implication of this is that we must impose a vertical scale on the problem. We can choose a boundary layer thickness or the depth of the water, but the vertical scale of the problem is not necessarily determined by (4).

For a derivation of such properties of (4) as vertical center of mass and accumulative mass fraction refer to Hannah et al. (1995), here we extend those derivations to the more general 2-layer formulation following Li and Amos (2001).

The 2-Layer Formulation

The 2-layer formulation takes into account the wave-current boundary layer. In this formulation, suspension is forced by u_{*cw} inside the wave-current boundary layer and u_{*c} above it (see Figure 5). u_{*cw} and u_{*c} are the total combined wave-current bottom stress and the total current bottom stress, respectively.

The 2-layer Rouse profile is a synthesis of 2 individual modified Rouse profiles (4) that merge at the interface of the two layers:

$$c(z) = \begin{cases} c_a(a/z)^{p_1} & z \leq \delta \\ \\ c_\delta(\delta/z)^{p_2} & z > \delta \end{cases} \tag{5}$$

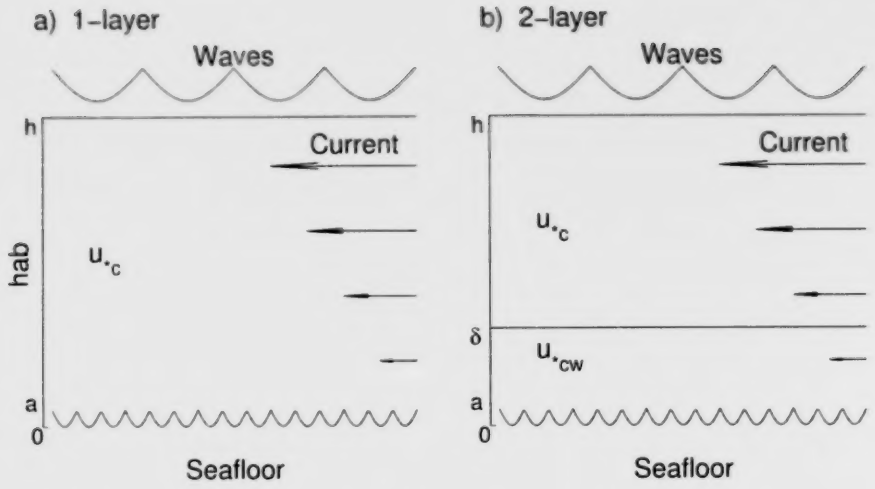

Figure 5: Depiction of a) 1-layer and b) 2-layer formulation. In the 1-layer case, a single bottom stress acts over the entire water column a to h. In the 2-layer case, the water column is divided into two layers: the wave-current and current, with u_{*cw} and u_{*c} acting in each.

where $\delta \geq a$ is the height of the current-wave boundary layer (Li and Amos, 2001), p_1 and p_2 are the Rouse numbers for the current-wave and current layers defined by

$$p_1 = \beta w_s/(\kappa u_{*cw}), \tag{6}$$

$$p_2 = \beta w_s/(\kappa u_{*c}). \tag{7}$$

where w_s is the settling velocity. β is an empirical scaling factor which is set to $\beta = 0.74$ for the 2 boundary layer case (Li and Amos, 2001; Grant and Madsen, 1986), and $\beta = 1.0$ for the single. From continuity it follows that

$$c_\delta = c_a(a/\delta)^{p_1}. \tag{8}$$

The next step is to derive an expression for c_a. Consider a case where the bottom shear stress is sufficient to suspend all the sediment. The total mass, M, in a vertical column of height h and unit cross-section, is the vertical integral of (5),

$$M = \int_a^\delta c_a(a/z)^{p_1} \mathrm{d}z + \int_\delta^h c_\delta(\delta/z)^{p_2} \mathrm{d}z \tag{9}$$

which serves to define c_a,

$$c_a = \frac{M}{a}[H(p_1, \frac{\delta}{a}) + \eta H(p_2, \frac{h}{\delta})]^{-1}, \tag{10}$$

where

$$H(p,v) = \begin{cases} \frac{1}{1-p}[v^{1-p} - 1] & p = 1 \\ \ln(v) & p \neq 1 \end{cases} \tag{11}$$

and

$$\eta = (\frac{\delta}{a})^{1-p_1}. \tag{12}$$

Define $F(z)$ as the fraction of the mass contained between the reference height a and the height z. All information about the vertical concentration profile is captured in $F(z)$ which is used as probability distribution function for the vertical profile and as part of the vertical mixing parameterization (Sections 3.4, 3.6 and Appendix D).

The expression for $F(z)$ is derived by integrating (5) from a to z and substituting (10):

$$F(z) = \frac{H(p_1, \frac{z}{a})}{A + \eta B}(1 - \Theta_\delta(z)) + \frac{A + \eta H(p_2, \frac{z}{\delta})}{A + \eta B}\Theta_\delta(z), \tag{13}$$

where $A = H(p_1, \frac{\delta}{a})$ and $B = H(p_2, \frac{h}{\delta})$, $\Theta_\delta(z)$ is the step function defined to be 0 for $z < \delta$ and 1 for $z \geq \delta$.

In the limit as $\delta \rightarrow a$, $A = 0$ and $\eta = 1$ which leads to

$$F(z) = \frac{H(p_2, \frac{z}{a})}{H(p_2, \frac{h}{a})}. \tag{14}$$

Likewise in the limit as $\delta \rightarrow h$,

$$F(z) = \frac{H(p_1, \frac{z}{a})}{H(p_1, \frac{h}{a})}. \tag{15}$$

Both expressions lead to the formulation of $F(z)$ in Hannah et al. (1995) depending on the choice of p_1 or p_2. The expressions for the mean and median height can readily be derived from (13) but are not included here since `bblt` only uses (13).

In order to simplify the appearance of equations in this section, the reference and maximum heights were referred to as a and h respectively. Elsewhere in this manual they are called h_{ref} and h_{max}.

The combination of continuous release and floc breakup (Section 3.3) allows for 2 distinct populations of packets, each with its own settling velocity. In this case `bblt v7.0` keeps 2 distinct versions of $F(z)$.

3.5 The Particle Model

A feature of `bblt` is the use of discrete pseudo-particles or "packets" rather than continuous concentrations to model the transport problem. The mass of material to be modelled,

M, is divided into N packets each with a mass $m =$ M/N. The model is formulated in Lagrangian coordinates, with the packet positions, $X_n(t)$, $Y_n(t)$ and $Z_n(t)$, as the basic output. There is no grid in the horizontal or the vertical. It is important to note that the packets are mathematical constructs with different vertical movement properties than real sediment particulates or flocs; rather, the net effect of their movement is intended to represent real-ocean shear dispersion. Some output quantities, such as concentration, are derived with a user defined grid.

The movement of the packets is divided into two parts: the vertical distribution and the horizontal transport. Given a time-dependent velocity field, an advection time step Δt_a, and a distribution of packets, the horizontal advection of the packets is straight-forward. The difficulties, both conceptually and numerically, are with the vertical distribution.

Vertical motions are not modelled explicitly; they are parameterized in terms of the Rouse profile (4). For our purposes, the concentration profile is a mathematical construct which contains the dependence of the vertical distribution on the bottom stress and the settling velocity of the particles. We interpret the concentration profile as a probability distribution which provides a way to assign the vertical positions to the packets consistent with the concentration profile. We assume that the profile is an equilibrium one, with no explicit time dependence. Time dependence occurs through the dependence of the concentration profile on time varying bottom stress.

We assume that the important features of the small-scale interactions between the sediment, the bottom, and the turbulence in the water column are captured by the vertical profile of the sediment concentration. This approach is consistent with the form of most available quantitative information on suspended sediment transport.

The use of equilibrium concentration profiles requires that the time scale for the vertical mixing of the suspended sediment be shorter than the time scale for changes in the bottom stress. For the purposes of this work we assume that the velocity field (and the bottom stress) evolves on tidal time scales, i.e., order of hours.

Vertical positions are computed as follows, assign each packet n a random rank α_n uniformly distributed in the interval $(0, 1)$. The vertical position of any packet is the solution z_n to the equation $F(z_n) = \alpha_n$ where $F(z)$ is the fraction of mass contained between h_{ref} and z defined in (13). Thus, we convert a uniform distribution to a Rouse distribution; a packet with $\alpha = 0$ is positioned at $z = h_{ref}$ and a packet with $\alpha = 1$ is positioned at $z = h_{max}$. During integration $F(z)$ is updated at each time step to reflect changes in the concentration profile. As the bottom stress changes the concentration profile expands and contracts and the vertical coordinates of the packets change in concert.

Vertical redistribution of the packets takes place through expansion and contraction of the profile and through vertical mixing. In the absence of vertical mixing there will be very little dispersion of sediment. As discussed in reference to Figure 3, shear dispersion requires shear in the currents and mixing across the shear. In `bblt` vertical mixing is not modelled explicitly. It is parameterized in terms of mixing (or shuffling) of the α_n. This

introduces a free parameter t_m. As discussed in Hannah et al. (1995) and in Appendix D, the shuffling of the α_n yields results consistent with shear dispersion theory and allows for reasonable interpretation of t_m in terms of Lagragian mixing time scales. The shuffling algorithm is the topic of the next section.

3.6 Vertical Shuffling

Vertical mixing is achieved through the shuffling of packet ranks α_n. The shuffling extracts the net effect of the shear dispersion processes without explicitly modeling the motions of individual packets (Appendix D and Hannah et al., 1995).

Shuffling occurs after each advection timestep Δt_a. The number of packets to be shuffled each time γ is determined by the fraction $\gamma = \mathrm{N}\ \Delta t_a / t_m$, where t_m is the vertical mixing timescale and N is the total number of packets. There are 4 shuffling algorithms in `bblt v7.0`:

1. **No vertical mixing.** No shuffling occurs. The packets maintain their relative vertical positions but their absolute vertical position can change as the bottom stress changes.

2. **Random pair-wise exchange.** At each advection timestep γ pairs of packets are chosen at random and their ranks swapped. This is the algorithm used in previous versions of `bblt`.

3. **Systematic pair-wise exchange.** In the time interval t_m, the list of packets is traversed exactly once and the α_n of each packet is swapped with the α_n of another packet in the list chosen at random (besides itself).

4. **Randomly assign new ranks.** At each advection timestep γ pairs of packets are chosen at random and assigned a new α_n drawn from the uniform distribution $(0, 1)$.

Figure 6 shows a pair-wise exchange that would be typical of a method using pair swapping (method 2 and 3).

Method 3 differs from 2 and 4 in that it guarantees that each packet will be shuffled at least once during t_m. To ensure that this happens, the list of packets is traversed once during t_m. To prevent any coupling between the periodicity induced by this method and that of the forcing (e.g. tidal period), the starting location in the packet list is chosen at random at the onset of each t_m cycle.

All 3 methods shuffle 2γ packets at each advection timestep. In the case of method 2 and 3, this consists of swaps of the α_n of γ packet pairs. In method 4, γ packet pairs are assigned new α_n drawn from $(0, 1)$; pairs are selected in order to achieve 2γ packet

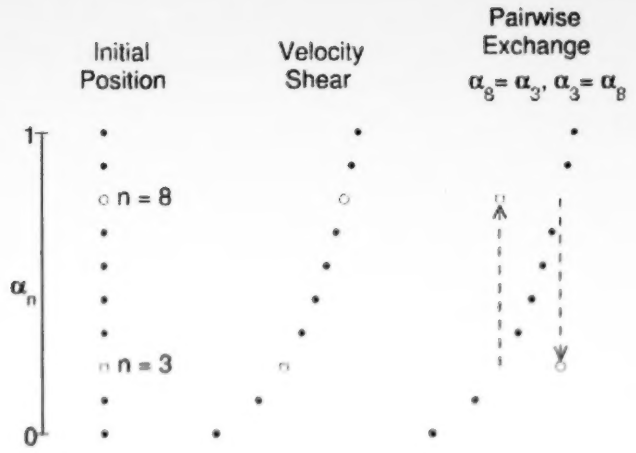

Figure 6: Schematic of shearing and shuffling of a vertical line of packets in a horizontal current. The packet ranks (α_n) are uniformly distributed in the interval (0,1). The exchange of ranks is performed at each advection time step, Δt_a, for $N\Delta t_a/t_m$ randomly selected pairs of packets. A packet with $\alpha = 1$ is located at h_{max} and a packet with $\alpha = 0$ is located at h_{ref}.

shuffles at each advection timestep as is the case with method 2 and 3. Method 4 differs further from 2 and 3, in that it causes the mean height of the distribution to fluctuate slightly. Appendix D.2 compares the properties of the 3 methods.

Not all shuffling algorithms yield reasonable results. For example, the original version of method 3, cycled through the list of packets in a systematic manner. The algorithm started at packet 1 and worked its way to packet N. Then it started back at packet 1. This gave an unexpected result. In a periodic flow, there would be no dispersion when t_m was equal to the flow period. This was due to a coupling between the flow reversals and the shuffling. This was not acceptable because in a general velocity time series dispersion due to some flow components would be lost. The fix was to start the shuffling sequence at a different location in the list of packets after each t_m interval.

3.7 Vertical Shear

The vertical shear of the currents is a critical factor in shear dispersion, which is the core process in `bblt`. In the interior of the water column, it is assumed that the velocity shear between the current meters is adequately captured by linear interpolation. If this is not sufficient, then prior knowledge must be used to create synthetic current time series (between the current meters) and these used as additional input to `bblt`.

The details of the near bottom velocity profile are important because most of the tidal current shear occurs here. A logarithmic profile is used to calculate the velocity below the

lowest (nearest to the bottom) current meter (this replaces the linear profile used in `bblt` v1). The logarithmic layer is an approximation of the turbulent boundary layer which generally extends a few metres above the seafloor. The lowest current observation should come from within this layer. Details of the implementation are provided in Appendix B.

Often the natural sediment concentration profile will extend higher into the water column than the upper current meter. In `bblt` the parameter h_{max} governs the maximum height of the concentration profile. Clearly h_{max} can not exceed the height of the upper current meter, since there is no velocity information above this height. The user can either accept this limitation or create synthetic time series higher in the water column. The technique of generating a synthetic time series by duplicating the upper current meter at a higher level (e.g. creating a time series at 20 m above the bottom which is identical to the observed currents at 10 m) creates a no shear zone which has an interesting side effect. In most cases the mean drift will be increased, but the mean diffusivity will be reduced because the mean shear in the water column has been reduced.

3.8 Biological Impact Module

The biological effects predicted by `bblt v7.0` are based on the results of laboratory experiments reported by Cranford and Gordon (1992), Cranford (1995) and Cranford et al. (1999) These experiments exposed sea scallops to different concentrations of various drilling wastes. Two thresholds were estimated from bentonite and barite exposure data: the no-observed-effects (C_0), and the no-growth (C_1) concentrations. For barite, $C_0 = 0.1$ mg $L^{-1}$and $C_1 = 0.5$ mg L^{-1}, while for bentonite $C_0 = 2$ mg $L^{-1}$and $C_1 = 10$ mg L^{-1} (Cranford et al., 2003). `bblt v7.0` computes the potential growth inhibition, PGI, in days (i.e growth days lost):

$$PGI = \Sigma_{i=1}^{N_t} R(t_i)/M_s, \tag{16}$$

where N_t is the the total number of timesteps for the period considered, t_i is the time at timestep i and M_s is the number of time steps per day. The reduction index $R(t)$ represents the fraction of potential growth time lost at a particular timestep and is limited to the range $[0, 1]$

$$R(t) = \begin{cases} gC(t) + b, & C_0 < C(t) < C_1 \\ 1, & C(t) \geq C_1 \\ 0, & C(t) \leq C_0 \end{cases} \tag{17}$$

with

$$g = (C_1 - C_0)^{-1}; \quad b = (1 - \frac{C_1}{C_0})^{-1}. \tag{18}$$

Only one drilling waste component is considered. The time dependence in $R(t)$ is parametrized through the concentration.

3.9 Model Output and Derived Quantities

The model outputs are the time series of positions of the packets

$$X_n(t),\ Y_n(t),\ Z_n(t) \quad \text{for} \quad n = 1, \ldots, \mathrm{N} \tag{19}$$

where N is the number of packets, $X_n(t)$ is the position along the x coordinate of packet n at time t, Y is the y coordinate and Z is the vertical coordinate (positive upwards from the sea floor). Everything else is a derived quantity. Here we define the basic derived quantities.

First we define the center of mass of the cloud of packets at time t $(\overline{X}(t), \overline{Y}(t), \overline{Z}(t))$ where

$$\overline{X}(t) = (1/\mathrm{N}) \sum_{n=1}^{\mathrm{N}} X_n(t) \tag{20}$$

and the other two components are defined in the same manner.

The mean drift (U, V) is the time rate of change of the horizontal center of mass over the simulation. U (V) is computed as the slope of a straight line fit to the time series $\overline{X}(t)$ $(\overline{Y}(t))$.

The horizontal spreading of the patch about its center of mass is measured by the horizontal variance of the packet distribution σ^2. In one dimension the variance of N packets is

$$\sigma^2(t) = \frac{1}{\mathrm{N} - 1} \sum_{n=1}^{\mathrm{N}} (X_n - \overline{X})^2 \tag{21}$$

In two dimensions we calculate σ^2_{max} and σ^2_{min} which are the variances along the major and minor axes of the horizontal projection of the distribution (i.e. the vertical coordinate is ignored). At each time, σ^2_{max} and σ^2_{min} are the eigenvalues of the covariance matrix

$$\zeta = \begin{bmatrix} \sigma^2_{xx} & \sigma^2_{xy} \\ \sigma^2_{xy} & \sigma^2_{yy} \end{bmatrix} \tag{22}$$

where

$$\begin{aligned} \sigma^2_{xx} &= \tfrac{1}{\mathrm{N}-1} \textstyle\sum_{n=1}^{\mathrm{N}} (X_n - \overline{X})^2 \\ \sigma^2_{yy} &= \tfrac{1}{\mathrm{N}-1} \textstyle\sum_{n=1}^{\mathrm{N}} (Y_n - \overline{Y})^2 \\ \sigma^2_{xy} &= \tfrac{1}{\mathrm{N}-1} \textstyle\sum_{n=1}^{\mathrm{N}} (X_n - \overline{X})(Y_n - \overline{Y}) \end{aligned} \tag{23}$$

The solutions are (Preisendorfer, 1988)

$$\begin{aligned} \sigma^2_{max} &= \tfrac{1}{2}[(\sigma^2_{xx} + \sigma^2_{yy}) + E] \\ \sigma^2_{min} &= \tfrac{1}{2}[(\sigma^2_{xx} + \sigma^2_{yy}) - E] \end{aligned} \tag{24}$$

where

$$E = [(\sigma_{xx}^2 - \sigma_{yy}^2)^2 + 4(\sigma_{xy}^2)^2]^{1/2}. \tag{25}$$

The effective horizontal diffusivities along the major (K_{max}) and minor (K_{min}) axes are then defined as

$$K_{max} = \frac{1}{2}\frac{\partial < \sigma^2{}_{max} >}{\partial t} \quad ; \quad K_{min} = \frac{1}{2}\frac{\partial < \sigma^2{}_{min} >}{\partial t} \tag{26}$$

(Csanady 1973) where $< \cdot >$ denotes a time averaging which smooths out short-term fluctuations such as the tides.

The interpretation of the mean drift and the horizontal diffusivity is straight-forward for bulk releases. These quantities are less meaningful for continuous scenarios.

Concentration

The calculation of concentration in `bblt v7.0` is based on counting packets in a user specified volume. There are 3 separate concentration calculations which differ in their sampling regions and/or computation schemes.

For the calculation of concentration following the center of mass (statistics file), the sampling region is a cylinder of radius r, centered at the center of mass of the packets and extending in the vertical from z_1 to z_2. The concentration is computed by counting the packets inside the sampling volume and multiplying by the ratio of the packet mass to the sampling volume. For the depth-integrated concentration (mass per unit area) the sampling volume extends over the entire water column.

The calculation of concentration at user specified positions is handled differently in order to improve the minimum resolvable concentration. The procedure is to calculate the depth-integrated concentration by packet counting and then infer the volumetric concentration from the vertical distribution (13). The calculation yields the average concentration between the user specified vertical positions z_1 and z_2. The only difference between the time series calculation and the concentration map calculation is that the first uses a disk of radius r while the latter uses a user defined rectangular grid.

Consider the minimum resolvable concentration (due to 1 particle) achieved by the two methods. For strict packet counting, the minimum resolvable concentration is

$$C_{\min} = \frac{m}{A(z_2 - z_1)} \tag{27}$$

where m is the mass of one packet and A is the horizontal sampling area. When the volumetric concentration is calculated from the depth-integrated concentration and the vertical structure, the minimum resolvable concentration is not a constant. It depends on the vertical position in the water column, the vertical distribution of the material and the minimum single particle depth-integrated concentration m/A. The upper bound for the minimum resolvable concentration is given by (27) The lower bound does not exist

in general, however for the near-bottom concentration, the lower bound is $m/(A(z_{max} - z_{ref}))$, and occurs when the sediment has a uniform vertical distribution. The inference procedure improves the minimum resolvable concentration by as much as 2 orders of magnitude in the near bottom region and the improvement can be even greater in the upper water column.

A feature of the inference method is that when there is at least one packet in the horizontal sampling area, there will be non-zero concentration over the entire water column. This is particularly noticeable in the case of high Rouse number, where the sediment is localized near the bottom. Counting packets in the upper water column would almost certainly yield a zero concentration (due to finite number of packets) however using the analytical expression always gives a non-zero value.

4 Software Overview

In this section, the `bblt v7.0` code is described. This description should help the user understand how `bblt` functions and aid in making modifications. The user may wish to modify the output modules (`Output`) and the modules that describe the interaction of the sediment with the bottom: the critical threshold stress (`Threshold`) and the fraction of the sediment in suspension (`SuspendedFraction`). The user may also wish to modify the input.

The computer code is written in FORTRAN77 and is reasonably portable. It has been compiled and run on both Windows and Linux platforms.

The program is organized as a main module which implements the algorithm shown in Table 1 and submodules (functions) which perform specific tasks. The modules are listed below in the order they are executed in the main loop and a brief description is given. Where the functional name is different than the file name, the functional name is bracketed.

`bbltv7.f` This is the main module for `bblt`. Here, most of the variables are initialized, time stepping is organized and error reporting is carried out. The main loop steps over each advection timestep calling the appropriate subroutines.

This file also contains `ErrorReport`, a module for writing error messages to both standard output and the echo file.

`UserSetup.f` A place for the user to open files and do other setup activity. It is called early in the initialization process. At present this module is empty.

`RdParams7.f (RdParams)` Reads the input parameters. Converts all time parameters to seconds.

Table 1: Outline of the algorithm for `bblt v7.0`. The symbols are defined in the text and in Tables 2 and Appendix A.

Define:

$q = \Delta t_U / \Delta t_a$ number of distinct advection steps (and mixing events) between updates of the velocity field. Δt_a is adjusted so that q is an integer

Initialize:

specify input parameters: t_m, Δt_a, Δt_U, t_s, t_t, etc.
$t = t_s$
initialize packets and create list of ranks (α_n)
get initial velocity field: $\mathbf{u}(t_s)$
get initial bottom stress: u_* and decide 1 or 2 layer formulation
initialize output

Main Loop:

do until time $t \geq t_s + t_t$
  get $\mathbf{u}(z, t + \Delta t_U)$
  do j = 1, q
    compute $\mathbf{u}(z, t)$ and u_* by interpolating
    create more packets if needed
    perform k pair-wise exchanges of the α_n
    decided settling velocity (breakup case only)
    compute rouse numbers
    compute the probability distribution $F(z)$
    compute vertical positions of packets: Z_n
    advect packets in the horizontal: (X_n, Y_n)
    output
  enddo
  $t = t + \Delta t_U$
enddo

`nodeinfo7.f (NodeInfo)` This subroutine uses the depths of the current meters and the user specified log-layer heights to construct a list of heights (or nodes) above the bottom where velocities are specified (page 27). A sample input file is shown in Appendix G.

`velinfo7.f (VelInfo)` On first call (initialization), reads names of the velocity files from the input, opens each velocity file and advances to the start time of the run (actually to the nearest time point, the code start time is adjusted to this value). A time stamp integrity test is perform in which the starting time of all vertical levels must fall within $\approx 45s \approx 0.0005$ days. The choice of tolerance is arbitrary and can be changed by the user in bbltCONST.h. The tolerance was picked because it made a time stamp in yeardays with 3 decimal places acceptable for the code. On subsequent calls, the routine updates the velocity field at each Δt_U and computes the velocity profile below the bottom velocity observation.

The calculation of the near-bottom velocity profile is based on the logarithmic profile described in Appendix B. The calculation assumes a quadratic stress law and the free parameter ξ_0 (roughness length) is hard-coded into the subroutine. The calculation of the logarithmic profile is separate from the calculation of the friction velocity (u_*) used to calculate the sediment concentration profile. In particular, changing the coefficients in the polynomial stress law (1) has no effect on the log-layer.

`InterpVel.f` Linearly interpolates velocity data from the velocity update time steps (Δt_U) to the advection time steps (Δt_a).

`stress_info7.f (StressInfo)` On first call (initialization), reads names of the friction velocity files from the input file, opens it and advances to start time of the run. A time stamp integrity test is perform in which the found starting time must fall within $\approx 45\ s \approx 0.0005$ days of model start time, which may have been modified by the `velinfo`. The point is that the velocity and bottom friction time series must have the same time stamp. On subsequent calls, the routine updates the friction velocity at each Δt_U.

`CalcUstar.f` Uses the velocity and specified friction parameters to calculate the friction velocity (u_*). Called only when friction velocity time series is not specified.

`SedFcns.f` A collection of functions related to the suspended sediment.

`Rousenum` Calculates the Rouse number from u_*, κ, w_s and β.

`Threshold` User defined critical shear velocity, u_{*crit}. Currently set to return 0 at all times leading to the suspended fraction always being 1.

`SuspendedFraction` User defined function which calculates the fraction of sediment in suspension based the critical shear velocity from above.

CrtPckts7.f (CrtPckts, CrtPcktsDis) On the first call (initialization), randomly generates α_n's for the maximum number of packets allowable (see bbltCONST.h). On subsequent calls, packets are activated as required for a continuous release or time series discharge scenario.

VertShff17.f (VertShuff1) Carries out the vertical shuffling as discussed in Section 3.6.

PDFcompute.f (PDFcompute, PDFcompute2, HH) Based on Rouse numbers and other vertical information, creates a table of cumulative probability ($F(z)$) at logarithmically spaced depths (smaller interval near the bottom). The number of values in the table is controlled by the variable **nentry** in this subroutine. The current value is **nentry=50** set inside bbltCONST.h. **PDFcompute2** handles the 2-layer case and uses the function **HH**. **PDFcompute** is called during a 1-layer run.

AbRVertPos7.f (AbRVertPos2) Adjusts the vertical position of the packets to fit the updated probability distribution. Based on the details of **PDFcompute**, material not in suspension is assigned a height $z = h_{ref}/2$. This allows the user to choose whether the material not in suspension is counted as part of the near-bottom concentration. The choice is made via the choice of the lower limit in the concentration calculation.

VelHoriz.f Calculates the velocity at the vertical position of a given packet using linear interpolation.

MoveHoriz.f Horizontal advection of packets. The movement is simply the drift of the particles due to the local current.

output7.f This module contains the subroutines listed below which initialize the standard output files and calculate and record the results at user specified intervals.

output Organize the calculation of the output and calls all the subroutines bellow.

outfileopen Open an output file

sedout Packet information

velout Velocity information

statout Standard statistics

packout Packet positions

controut Time series of concentration at specified locations

contrmaout Concentration maps

Cncentr1 Calculate concentration (used by **controut**).

biologyout Growth days lost at specified locations

biologymapout Concentration maps of growth days lost

PDFatZ Interpolates table of cumulative probability.

`ranf1.f` Contains subroutines used by the random number generator. The random number generator used by `bblt v7.0` is a part of the **RANLIB** package compiled by Barry W. Brown, James Lovato and Kathy Russell (available from `http://www.netlib.org`). It is based on the algorithm of L'Ecuyer and Cote (1991) and has a period of 2.3×10^{18}.

`inputStyleRoutines.f` Routine decides the method used to read the input file. The input file name can either redirected via standard input at command prompt or supplied as an argument after the `bblt` executable at command prompt. The output is redirected to a file if a file name is supplied for the second argument. Otherwise the output is sent to standard output.

`nextpointer.f` A function that returns the next available file pointer number. It is used to assign Fortran logical unit numbers (LUN) to files being opened.

`h-files` All relevant variable in `bblt v7.0` are declared in h-files and shared by means of common blocks. Below is a brief account.

```
bbltCONST.h:      all constants
bbltIO.h:         reading and writing
bbltprog.h:       progress report indicator
bbltran.h:        random numbers
biologyIN.h       biology input
biologyOUT.h      biology output
contrIN.h         concentration time series input
contrmapIN.h      concentration map  input
contrmapOUT.h     concentration map  output
contrOUT.h        concentration time series output
discharge.h       packet discharge information
frictionIN.h      friction inputs
frictionMID.h     intermediate friction variables
heightIN.h        height inputs (hmax, href)
packets.h         packets information
packIN.h          inputs for pack position file
PDFvi.h           cumulative particle fraction
positions.h       packet positions
ranks.h           ranks
releaseIN.h       packet release input
rouse.h           rouse numbers
sedIN.h           inputs for sediment file
settlingIN.h      settling velocities input
settlingMID.h     intermediate settling variables
shufflingIN.h     shuffling inputs
shufflingMID.h    intermediate shuffling variables
statsIN.h         inputs for statistics file
```

timingIN.h	timing inputs
timingMID.h	intermediate timing variables
velinfoIN.h	velocity information inputs
velinfoMID.h	intermediate velocity information variables
velocityIN.h	inputs for velocity file
velocityMID.h	intermediate velocity variables

Graphical User Interface

The graphical user interface (GUI) for bblt v7.0 was written in Java 1.4. The graphics were implemented using a free Java class library JFREECHART Version 0.9.15, written by David Gilbert and others. The library is available from http://www.jfree.org/jfreechart/index.html.

Included below is the list of java source files available with the current distribution of the bblt GUI:

BBLTAction.java	InputFields.java
BBLTGUI.java	InputPanel.java
BBLTPanel.java	LoadAction.java
BBLTProgressFrame.java	LoadBBLTFile.java
BBLTSetup.java	ModifiableProperties.java
BiologyAction.java	MyProperties.java
BiologyMapAction.java	NewAction.java
BiologyMapDemoGraph.java	OpenAction.java
BiologyMapGraph.java	OutputFields.java
BottomStressGraph.java	OutputGraphAction.java
BreakupAction.java	OutputPanel.java
BrowseAction.java	OutputTextAction.java
ButtonPanel.java	PositionAction.java
ConcentrationAction.java	ProgramInteractor.java
ConcentrationFrame.java	RandomAction1.java
ConcentrationGraph.java	RandomAction2.java
ConcentrationMapAction.java	RandomIntGenerator.java
ConcentrationMapOptionsFrame.java	RunAction.java
ConcentrationNumberAction.java	RunBBLT.java
ConcentrationParameters.java	SaveAction.java
CurrentRecordFilesAction.java	SedimentAction.java
CurrentRecordFrame.java	SedimentGraph.java
CurrentRecordsPanel.java	SedimentOptionsFrame.java
CurrentsGraph.java	SimpleFilter.java
DischargeAction.java	StatisticsAction.java
DischargeGraph.java	StatisticsGraph.java
DoubleFilter.java	StatisticsOptionsFrame.java
ExitAction.java	StreamReaderThread.java

FileInteractor.java
FrictionParametersAction.java
Graph.java
HelpAction.java
VelocityAction.java
VerAction.java
VerticalShufflingAction.java
VListSetup.java

5 Input Parameters

The input parameters describing the physics of a bblt simulation were discussed in Section 3. A detailed description of input parameters is provided here. Table 2 lists the symbols of parameters encountered in the text that are bblt v7.0 inputs. The relationship among the various time parameters is illustrated in Figure 7. In order to establish a connection between the general material presented here and the specific example given later, this section contains forward references to Section 6.

5.1 General Description

Velocity field Concurrent time series of easterly (u) and northerly (v) velocity at several vertical positions in the water column are required; ideally at least one vertical position should be within the bottom boundary layer. It is very important that the velocity time series are temporally aligned and have a uniform timestep (Δt_U). Once bblt finds the beginning of the time series (as determined by the start time t_s) it does not check the time stamps again.

As mentioned earlier, the source of the velocity data does not matter, it can be from current meters or numerical models. We refer to current meters for convenience.

Particle settling velocity The settling velocity, w_s, constant or stress dependent, should match that of the suspended sediment as discussed in Section 3.3. In the stress depended case, w_s takes on one the value of w_0, w_1, or w_2, depending on u_*^c. It is important to note that at times when $u_* < u_*^c$, newly added packets will have w_0 for their settling velocity while others w_1. On the other hand when $u_* \geq u_*^c$, all particles are broken up and have w_2 for their settling velocity.

The predicted dispersion and transport of sediment are strongly dependent on w_s and in circumstances where it cannot be well defined a sensitivity analysis should be performed.

Maximum height of sediment profile Typically the bottom boundary layer is restricted to a few 10's of meters above the sea floor. Often the bottom boundary layer is restricted by stratification in the water column. The user must specify the maximum height (h_{max}) of the concentration profile. bblt sets h_{max} to the minimum of the user specified h_{max} and the height of the upper current time series.

Table 2: List of `bblt v7.0` input parameter symbols. Note: this table defines only the symbols of input parameters used in the text. For a complete description of `bblt v7.0` input parameters see Section 5.2. For a list of all other symbols used in the text see Appendix A

$u(z,t)$, $v(z,t)$	the East and North velocity field components ($\mathrm{m\,s^{-1}}$)
w_0, w_1, w_2	initial, natural floc and after-breakup settling velocities ($\mathrm{m\,s^{-1}}$)
u_*^c	Critical friction velocity for breakup ($\mathrm{m\,s^{-1}}$)
u_{*c}	total(skin plus bed) currents friction velocity ($\mathrm{m\,s^{-1}}$)
u_{*cw}	total(skin plus bed) currents and wave friction velocity ($\mathrm{m\,s^{-1}}$)
δ	height of current-wave boundary layer (m)
h_{max}	maximum height of suspended sediment (m)
h_{ref}	sediment reference height (m)
$a_0, a_1, \ldots, a_n$	bottom friction parameters
$\kappa = 0.4$	von Karman constant
N	number of packets
M	total mass of packets (g)
m	the individual packet mass (g)
t_m	vertical shuffling time scale (h)
Δt_a	advection time step (h)
Δt_U	time between updates of the velocity field (h)
Δ_{rel}	The time step for continuous release (h)
t_{rel}	the total duration of continuous release (h)
t_s	start time of the simulation (year-days)
t_t	total duration of the simulation (h)
C_0	the no-observed-effects concentration ($\mathrm{mg\,L^{-1}}$)
C_1	the no-growth concentrations ($\mathrm{mg\,L^{-1}}$)
ξ_s	user specified log-layer heights (m)
N_{sl}	total number of user specified log-layer heights

Sediment reference height The sediment reference height (h_{ref}) is a mathematical construct which defines the lower boundary of the suspended sediment load in the Rouse profile. h_{ref} must not be less than the roughness height (ξ_0) used in the log-layer calculation (Appendix B) and a typical value for `bblt` applications has been 0.35 cm.

Bottom stress The friction velocity u_* is read from a file or computed from the near-bottom currents using a polynomial stress law. It is also important to note that `bblt` calculates a drag coefficient separately for extrapolation of the currents below the bottom current meter record (Appendix B).

Number and mass of packets The mass of material to be modelled, M, is divided into N equal packets.

Packet discharge time series The user can specify a time series of packet discharges. One of the headers in this file must be the individual packet mass. An example of this file is included in Appendix F.2.

Vertical shuffling time scale The vertical shuffling time scale, t_m, is the time required to do N pair-wise packet exchanges, or 2N random rank reassignments, depending on the shuffling algorithm. The shuffling time scale is proportional to the vertical mixing time scale (average time for a particle to sample the entire vertical profile; Hannah et al., 1996). For $t_m \approx 3$ hours, dispersion is maximized for semi-diurnal forcing. In one set of realistic simulations, the net dispersion varied by roughly a factor of 2 for t_m in the range of 1 to 10 hours.

Advection time step The advection time step, Δt_a, is the length of time between updates of currents, friction velocity and packet positions. At each advection time step, before horizontal advection takes place, $\gamma = N t_a / \Delta t_m$ pair-wise packet shuffles are performed and the vertical profile is fitted to the Rouse profile. `bblt` requires that $\Delta t_a \leq \Delta t_U$. In addition, it requires that $q = \Delta t_U / \Delta t_a$ be an integer (Table 1). `bblt v7.0` adjusts the user specified Δt_a to achieve this. Further N, Δt_a and t_m must be chosen in such a way that at least 1 vertical shuffle takes place at each Δt_a. The program stops if this is not the case. The input velocity and friction velocity time series (with time interval Δt_U) are interpolated to the advection time. Figure 7 illustrates relationship among the various time parameters.

Hannah et al. (1995) showed that dispersion is independent of Δt_a for $t_m > 2\Delta t_a$. For $t_m < 2\Delta t_a$ the granularity of the advection and the mixing becomes evident. The advection time step controls run time and $\Delta t_a = 0.1$ hrs is used in the sample run.

Start time The start time, t_s, is used as a pointer into the specified velocity time series. Each time series is searched until a record is found with time greater than or equal to $t_s - \Delta t_U/2$. The next record is the first one used and defines the start time. Thus the start time is modified to the nearest time point in the velocity file.

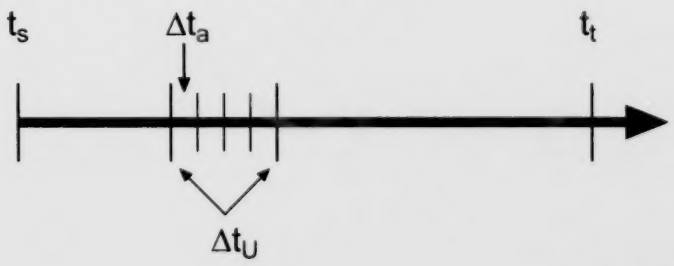

Figure 7: Schematic time line showing the relationship among t_s, t_t, Δt_a, and Δt_U.

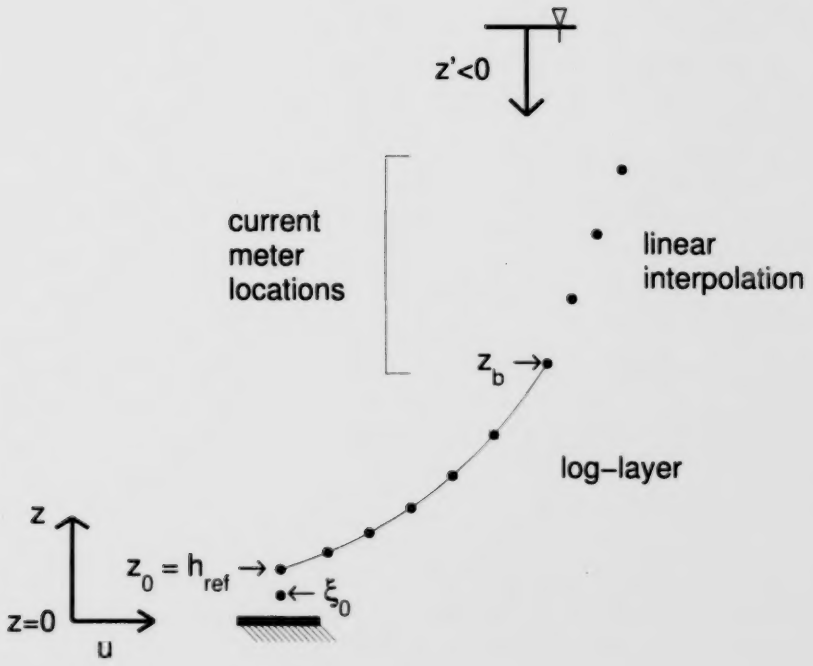

Figure 8: The water column as seen by `bblt`. The vertical coordinate is schematic and not to scale.

Total time The total integration time, t_t, controls the length of the simulation.

Another set of inputs is required to describe the vertical locations where the velocity field will be specified and/or calculated. Here we give some background on the requirements. A detailed example and explanation is provided for the sample run in Section 6.

The user must specify the currents at several vertical locations in the water column. While `bblt` works in terms of distance above the bottom, the vertical positions of the current meters are specified with respect to the surface of the ocean. The locations are described in a coordinate system (z') that is zero at the surface and positive upwards so the current meter locations are generally negative (Figure 8 and Appendix G.2).

The connection between the specified vertical locations, and the bottom of the ocean is provided as part of the specification of the near-bottom log-layer. The log-layer is a user specified set of vertical points given as heights above bottom. This information is to be provided in the log-layer file (e.g. Appendix G.1). `bblt` calculates currents at these location (Appendix B). The height above bottom of the lowest current meter coincides with the top of the log-layer. Thus the depth of the current meters and the height above bottom of the lowest current meter define the total water depth and the height of all the current meters (Figure 8). The total water depth is part of the standard output. Local

`bblt` assumes a constant depth ocean and does not account for changing depth due to processes such as waves.

The bottom of the log-layer, z_0, (Figure 8) specifies the minimum height above the bottom where the currents are calculated. `bblt v7.0` requires that $z_0 = h_{ref}$. A third near-bottom length scale is the roughness length ξ_0 from the log-layer calculation, `bblt v7.0` requires $\xi_0 < h_{ref}$. The program stops if these conditions are not satisfied.

Running `bblt` requires other parameters. For example, 2 seeds are required for the random number generator, a number is required to specify the method used for vertical shuffling and there are many input parameters required to control the output. These are described below and examples are given in Section 6 as part of the sample run.

5.2 Parameter Input File

This section contains a line by line description of the `bblt v7.0` input file. For an example see Appendix E. In this section we also introduce the graphical user interface (GUI) in conjunction with specific line inputs. Figure 9 contains a cross-reference for matching specific line numbers below with the GUI input text windows(labeled alphabetically).

Line 1 (GUI: P) All of the start-up information that appears on the screen during the run as well as additional information is sent to the echo file. If the file is to be saved in a directory other than the one in which the program is run, then the path should be specified as well. This is true of all the files in the input file.

Line 2 (GUI: A) Two numbers are required to seed the random number generator. The numbers used should be on the order of 2^{32}. Note that a given seed will always produce the same sequence of random numbers, so two model runs with the same input will produce identical output.

Line 3 (GUI: C) The duration of the run (t_l) and the start time of the run (t_s) are specified here. Units must be paid very close attention. The start time for the simulation is given in days, same as the time stamp in the velocity file. Other time-related input parameters are given in hours. `bblt` works internally in seconds.

Line 4 (GUI: D) The time between velocity updates (Δt_U) is the interval between velocity measurements in the velocity time series. It must be given in hours. The code does not check for consitency between Δt_U and the time step in velocity file. Care must be taken to ensure there are no gaps in the velocity files and that the time step matches Δt_U.

Line 5 (GUI: E) The advection time step (Δt_a) and vertical shuffling time scale (t_m) are specified in hours.

Line 6 (GUI: F) The method number, `vm`, to use for vertical shuffling. If `vm` = 1 there is no shuffling. If `vm` = 2,3 or 4 then the packets are shuffled γ times every advection time step using the selected mixing algorithm.

Line 7 The number given here tells `bblt` how many friction parameters will follow on line 8. If there are three friction parameters, then the friction velocity calculation is defined by a 2nd order polynomial. If 0,-1, or -2 is specified the following line will be read as the filename of the friction velocity file. Error will result for all other input values In the GUI, this line corresponds to the `Bottom Stress File` check box.

Line 8 (GUI: J) Either the friction velocity filename or the friction parameters (a_i) are read as determined by line 7. A sample friction velocity file is given in Appendix F.1 with a description of the format. Section 6.1 also describes this file in the context of an example.

There are 3 possibilities for the friction velocity file.

`if line 7 is -2 bblt` will work in the 2-layer mode, expecting a 4 column file. The columns must be: time (year days), u_{*cw} ($\mathrm{m\,s^{-1}}$), u_{*c} ($\mathrm{m\,s^{-1}}$) and δ (m). If less then 4 columns are provided an error will occur.

`if line 7 is -1` Works in 1 layer mode using the first column for time and the third column for u_*. If less then 3 columns are provided for this choice, an error will occur.

`if line 7 is 0` Works in 1 layer mode using the first column for time and the second column for u_*. Extra columns are ignored.

It's important to insure that there are no gaps in the data, and that the interval between data points is constant (and equal to Δt_U). Also the times must coincide (within $\approx 45s$) with that of the velocity (line 16).

For the case when a time series is not provided (i.e line 7 is greater then 0), The a_i parameters are listed from zeroth to $(n-1)$th order where n is the number of friction parameters (Line 7).

In the GUI, these options are made with the use of the `Bottom Stress File` check box and by choosing one of 3 model types: 2 layer, 1-layer (u_{*cw}) and 1-layer (u_{*c}).

Line 9 (GUI: K) The settling velocity parameters of the packets in $\mathrm{m\,s^{-1}}$. The four parameters are: w_0, w_1, w_2 and u_*^c. They are the initial, natural floc and after-breakup settling velocities as well as the critical friction velocity for breakup. If a constant settling velocity case is desired, the user must set $u_*^c < 0$. The GUI has a checkbox for breakup.

Line 10 (GUI: H) This line must contain two inputs: the von Karman constant $\kappa = 0.4$, and the reference height, h_{ref} (m). All lengths in `bblt` have units of metres. In GUI, the von Karman constant is automatically set to 0.4.

Line 11 (GUI: I) The maximum height of the sediment profile (h_{max}) is positive, and given in meters above the bottom. Current meters above this height are generally ignored. However, if h_{max} falls between 2 current depths, the the current meter closest to but higher than h_{max} is used for interpolation purposes. If h_{max} exceeds the height of the shallowest current meter then an error occurs.

Line 12 Selects the type of mass input for the following line. 0 = reads discharge file name while 1 = reads mass information. In the GUI, this option is incorporated in the `Discharge File` check box.

Line 13 (GUI: L) Reads the discharge filename or the information for a simple discharge. A sample of discharge file is given in Appendix F.2. Section 6.1 also describes this file in the context of an example.

If no discharge file is available, the mass information consists of four inputs. Four numbers are used to describe the scenario: 1) the total mass of material, M (g); 2) the total number of packets, N; 3) the release step Δ_{rel} (h); and 4) the total release time t_{rel} (h). `bblt` will release $N/(t_{rel}+1)/\Delta_{rel})$ packets every Δ_{rel} starting at the first advection step and finishing at time = t_{rel} for a total of N packets. If $t_{rel} \leq 0$ then all N packets are release at the start (bulk release).

Line 14 (GUI: M) This line gives the name of the file containing the heights in the log-layer (log-layer file) where velocities are to be calculated. In the example given in Appendix G.1, the heights are roughly logarithmically spaced. The heights must range from h_{ref} to the height of the bottom current measurement, which in the example is 3 meters. Since linear interpolation is used to calculate the velocities between the specified locations, high resolution is required to approximate a log-layer. Note that if there are only two heights, h_{ref} and the height of the bottom current meter, a linear boundary layer will result.

Line 15 (GUI: N) The file specified here contains the depths of the current meters. An example is given in Appendix G.2. The ordering of the depths is important. The depths must be ordered from the bottom up. The coordinate system is positive upwards with zero at the sea surface, so the depths are negative.

Line 16 In the lines after line 15, the files containing the velocity information are specified. The number of lines depends on the number of records. The number and order must correspond with the depths given in the file in Line 15. A sample velocity file is given in Appendix F.3. It's important to make sure that there are no gaps in the data, and that the interval between data points is constant (and equal to Δt_U).

In the GUI, current meter files are specified in an input window activated by pressing the `View Current Records` button (Figure 11).

The rest of the lines relate to model output. All output data files have an associated time step. In most cases the time step determines when to write the data to the ouput file. The exceptions are the two biological impacts modules where it determines the internal integration time step and output is only produced at the end of the simulation. In all cases, a time step of zero results in no output being produced and all subsequent lines related to that particular output must be omitted. When the timestep is smaller then Δt_a but non-zero, `bblt` resets it to Δt_a. All time steps are in hours. Output files are further discussed in Section 6.2

In the case of the concentration time series and the map, a negative time step indicates that the calculation is to be performed but not written to file. The calculation is performed with the absolute value of the time step provided. This option would typically be used when biological impact output is desired but not the concentration.

Line 17 (GUI: Q2) This line is the time step for the sediment parameters file.

Line 18 (GUI: Q1) Name of sediment parameters file (Section 6.2.1). An example of this file and its current format is given in Appendix H.1. The file format is defined by the module `sedout`.

Line 19 (GUI: Q2) The time step at which to output information about the velocity field.

Line 20 (GUI: Q1) The name of the file in which to store velocity information. The present file format is described in Section 6.2.2. The file format is defined by the module `velout`.

Line 21 (GUI: S2) The time step for statistics output.

Line 22 (GUI: S1) The name of the statistics file (Section 6.2.3). Sample output is reported in Appendix H.2. The file format is defined by the module `statout`.

Line 23 (GUI: S3-S5) This line gives the dimensions of the sampling cylinder for the statistics file. Expected are the height (above the bottom) of the bottom and top of the cylinder and the radius, all in metres. The bottom of the cylinder would typically be at the reference height if computing the near-bottom concentration, which is typically of concern. Other choices are possible. For details of the statistics calculation see Section 3.9.

Line 24 (GUI: T2) The time step for the packet positions $X_n(t)$, $Y_n(t)$ and $Z_n(t)$.

Line 25 (GUI: T1) The name of the file in which to store the packet position information. The file format is defined by the module `packout`. The format is described in Section 6.2.4. This can be a very large file and usually not useful. To avoid writing this output, set line 24 to zero.

Line 26 (GUI: U2) Time step for the concentration time series.

Line 27 (GUI: U1) The name of the file in which to store the concentration time series (Section 6.2.5). The file format is defined by the module `controut`. An example is given in Appendix H.3.

Line 28 (GUI: U3) The number of locations at which to record concentration time series.

Line 29 The locations and sampling volumes are listed in the lines following Line 28. There must be as many locations and sampling volumes as specified above. The first two numbers are the easterly- and northerly- coordinates relative to the release point (0,0), and the third is the radius of the cylinder. The last two numbers are the bottom and top of the cylinder. These are all given in meters. To calculate the near-bottom concentration of the suspended sediment, the bottom of the cylinder should be set to h_{ref}.

Figure 15 shows the window of the GUI where the information about concentration position and sampling volume is entered.

Line 30 (GUI: V2) Time step for the concentration maps.

Line 31 (GUI: V1) The output file name for concentration maps. The format is described in Section 6.2.6 and a sample concentration map is shown in Figure 16. The file format is defined by the module `contrmaout`.

Line 32 (GUI: V3-V10) The grid is defined on this line. The order is as follows: the number of grid points in the easterly direction followed by the minimum and maximum values, the number of grid points in the northerly direction followed by the minimum and maximum values and the bottom and top of the cylinder. All lengths are in meters.

Line 33 (GUI: W2) Time step for the biological impacts calculation.

Line 34 (GUI: W1) The output file name for the biological impacts calculation (Section 3.8 and 6.2.7). Sample output is reported in and Appendix H.4. The file format is defined by the module `biologyout`.

This calculation uses the concentration time series output (line 29).

Line 35 (GUI: W3-W4) This line defines the no-effects and no-growth concentration for the biological impacts calculation (Section 3.8).

Line 36 (GUI: Z2) Time step for the biological impacts map.

Line 37 (GUI: Z1) The output file name for biological impacts map. The format is described in Section 6.2.8 and a sample biological impacts map is shown in Figure 17.

The file format is defined by the module `biologyout`. The biology map uses the grid defined for the concentration map.

Line 38 (GUI: Z3-Z4) This line defines the no-effects and no-growth concentration for the biological impacts map output.

6 Sample `bblt` run

This section demonstrates the use of `bblt v7.0`. It can be run at the command line or with the `bblt v7.0` Graphical User Interface (GUI). The example described here is a simulation of drilling discharge at the North Triumph drilling site on Sable Island Bank. The simulation begins on 3 Oct. 1999, and lasts a total of 900 hours.

The particulars of the inputs and outputs are discussed in the context of the GUI. Appendix E contains the actual input file read by `bblt v7.0`. Appendix F contains fragments of the input time series: current meters, friction velocity and discharge. The log-layer and height files are included in Appendix G.

6.1 Input

The input file is shown loaded into the GUI (Figure 10). The sample input file is included in Appendix E.

This simulation uses 8 velocity records, a discharge time series and a friction velocity time series. Samples of these files are included in Appendix F. The GUI velocity file input window is shown in Figure 11. The GUI has the capability of displaying the input text files in a window and making plots. Figure 12 contains the GUI plots of the time series for the North Triumph example.

The auxiliary height and log-layer files (lines 13 and 14 Section 5.2) required by `bblt` for this simulation are shown in appendix G.

6.2 Output

In this section we take a detailed look at the output produced by a `bblt v7.0` run using the inputs described in the previous section.

Figure 9: Graphical user interface input file cross-reference. Text input windows are both labeled alphabetically and include the corresponding line numbers for the input file (Section 5.2 and Appendix E).

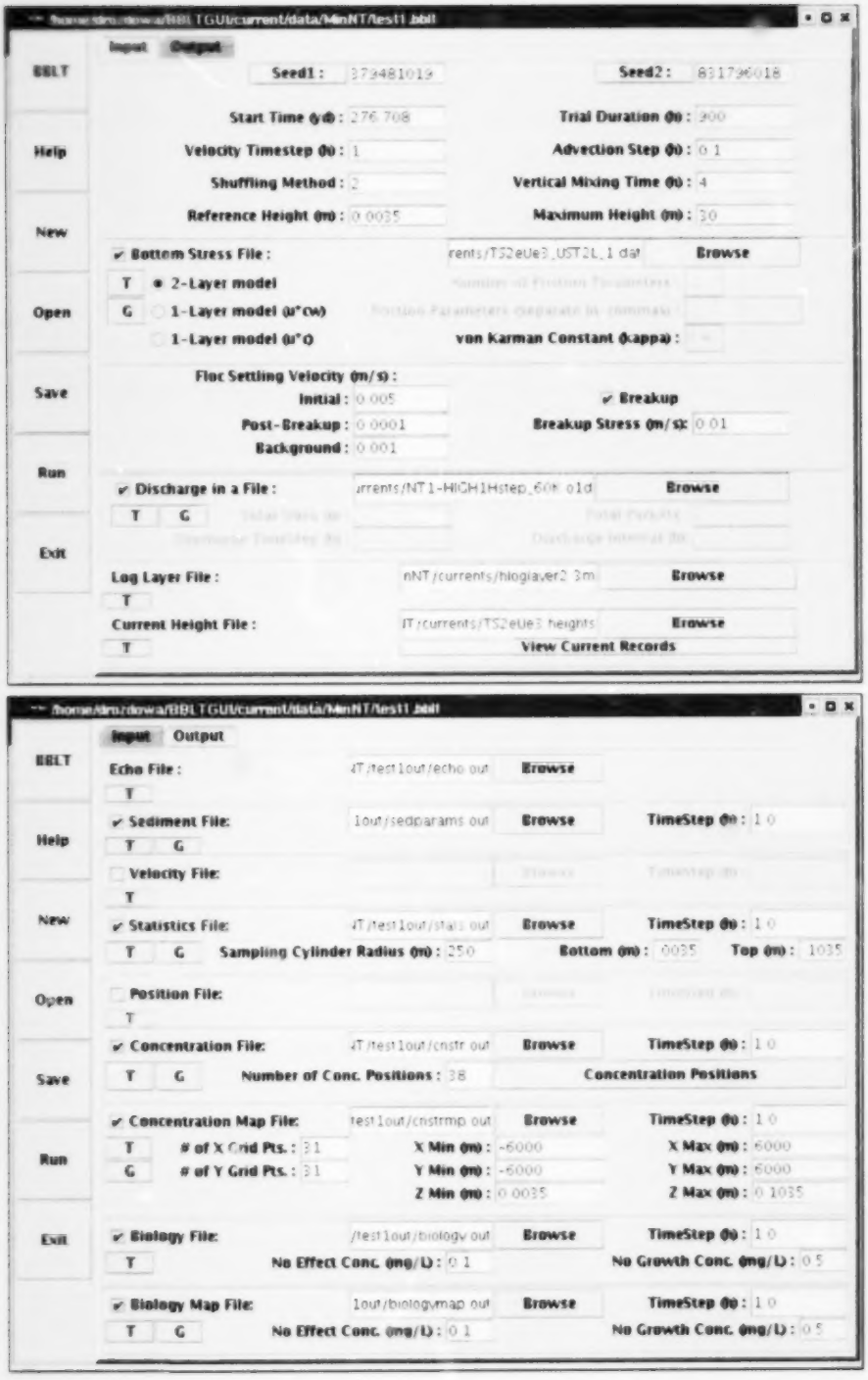

Figure 10: Graphical user interface input (top) and output (bottom) windows showing the North Triumph example.

Figure 11: Velocity file input window loaded with the North Triumph example.

Table 3: The four Rouse numbers calculated by `bblt v7.0` at each timestep and written to the sediment file. These are used by `bblt` at various times during computation, and are distinguished here by the parameters used to compute them.

Rouse Num.	u_*	w_s
p_1	u_{*cw}	w_1 or w_2
p_{1in}	u_{*cw}	w_0
p_2	u_{*c}	w_1 or w_2
p_{2in}	u_{*c}	w_0

6.2.1 Sediment parameters file (Line 17-18, GUI: Q1-Q2)

The sediment parameters file contains information about the calculated bottom shear velocity, Rouse profile, packet information and settling velocity. Appendix H.1 contains a sample. Figure 13 contains the GUI option screen for plotting various columns of the sediment file, along with a plot of Rouse numbers.

The first 8 columns of the output file are time (days), u_{*cw}, u_{*c}, δ, p_1, p_{1in}, p_2 and p_{2in} (See Table 3). The next 2 columns contain N, the total packets and N_b, the packets that have experienced breakup at least once. The last column contains the settling velocity of the N_b packets. The module that generates this file is `sedout`.

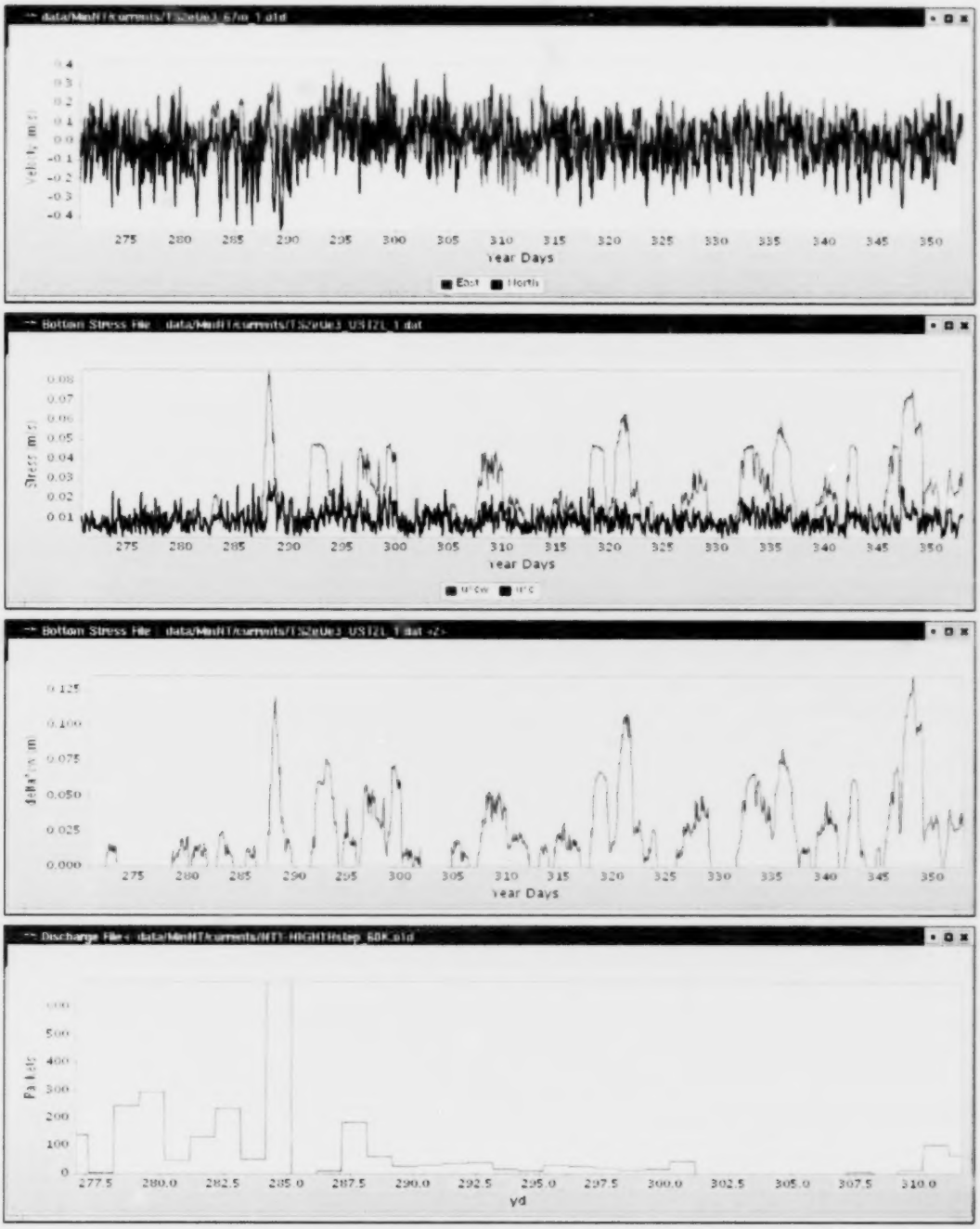

Figure 12: GUI plots of input time series. Starting from the top, current meter at 67m depth, friction velocity, boundary layer height and discharge.

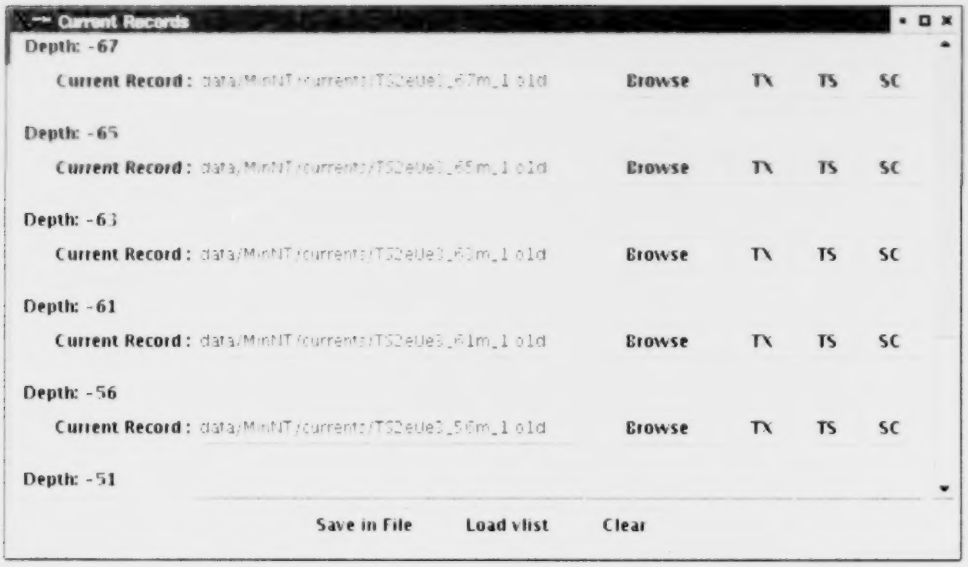

Figure 11: Velocity file input window loaded with the North Triumph example.

Table 3: The four Rouse numbers calculated by `bblt v7.0` at each timestep and written to the sediment file. These are used by `bblt` at various times during computation, and are distinguished here by the parameters used to compute them.

Rouse Num.	u_*	w_s
p_1	u_{*cw}	w_1 or w_2
p_{1m}	u_{*cw}	w_0
p_2	u_{*c}	w_1 or w_2
p_{2m}	u_{*c}	w_0

6.2.1 Sediment parameters file (Line 17-18, GUI: Q1-Q2)

The sediment parameters file contains information about the calculated bottom shear velocity, Rouse profile, packet information and settling velocity. Appendix H.1 contains a sample. Figure 13 contains the GUI option screen for plotting various columns of the sediment file, along with a plot of Rouse numbers.

The first 8 columns of the output file are time (days), u_{*cw}, u_{*c}, δ, p_1, p_{1m}, p_2 and p_{2m} (See Table 3). The next 2 columns contain N, the total packets and N_b, the packets that have experienced breakup at least once. The last column contains the settling velocity of the N_b packets. The module that generates this file is `sedout`.

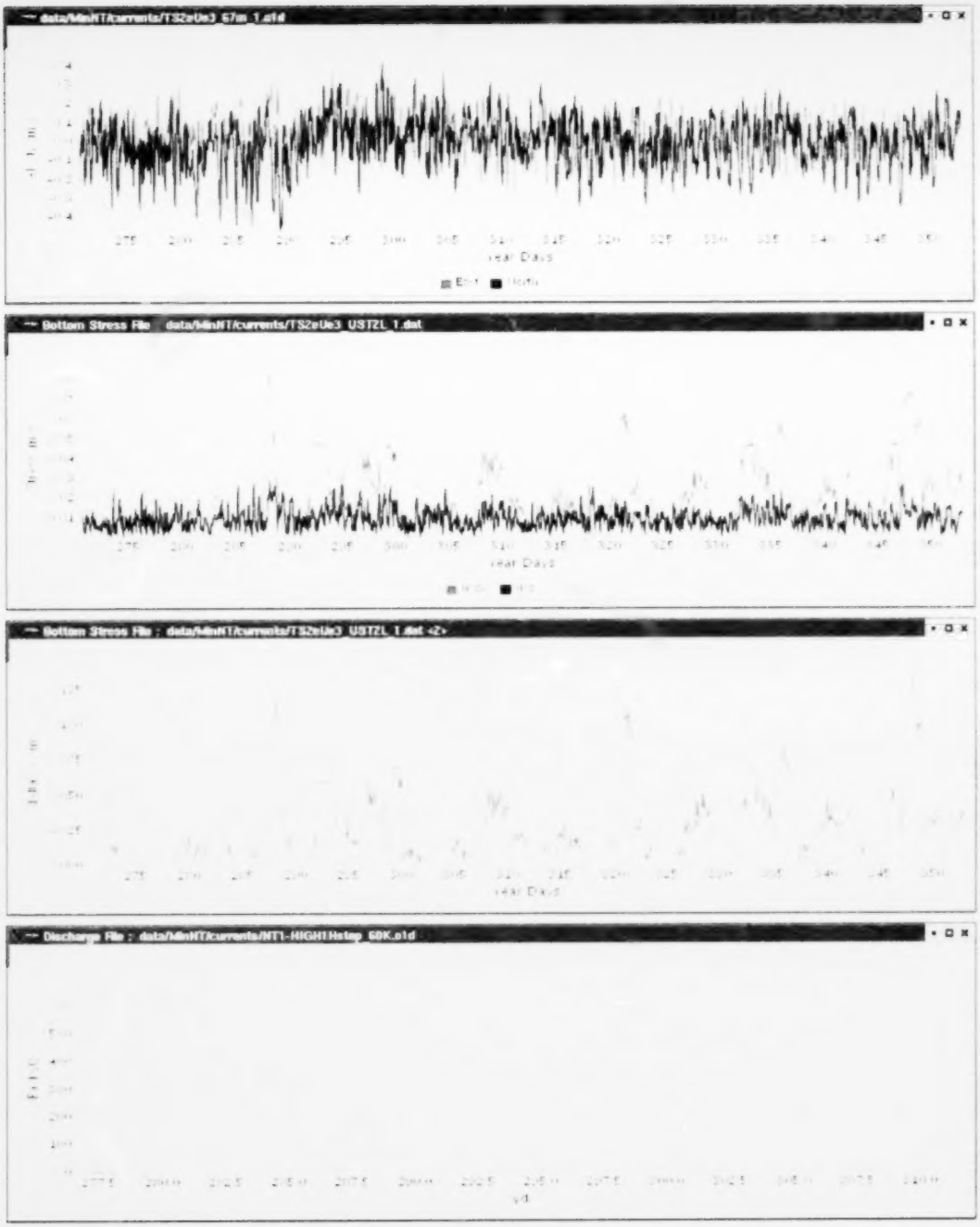

Figure 12: GUI plots of input time series. Starting from the top, current meter at 67m depth, friction velocity, boundary layer height and discharge.

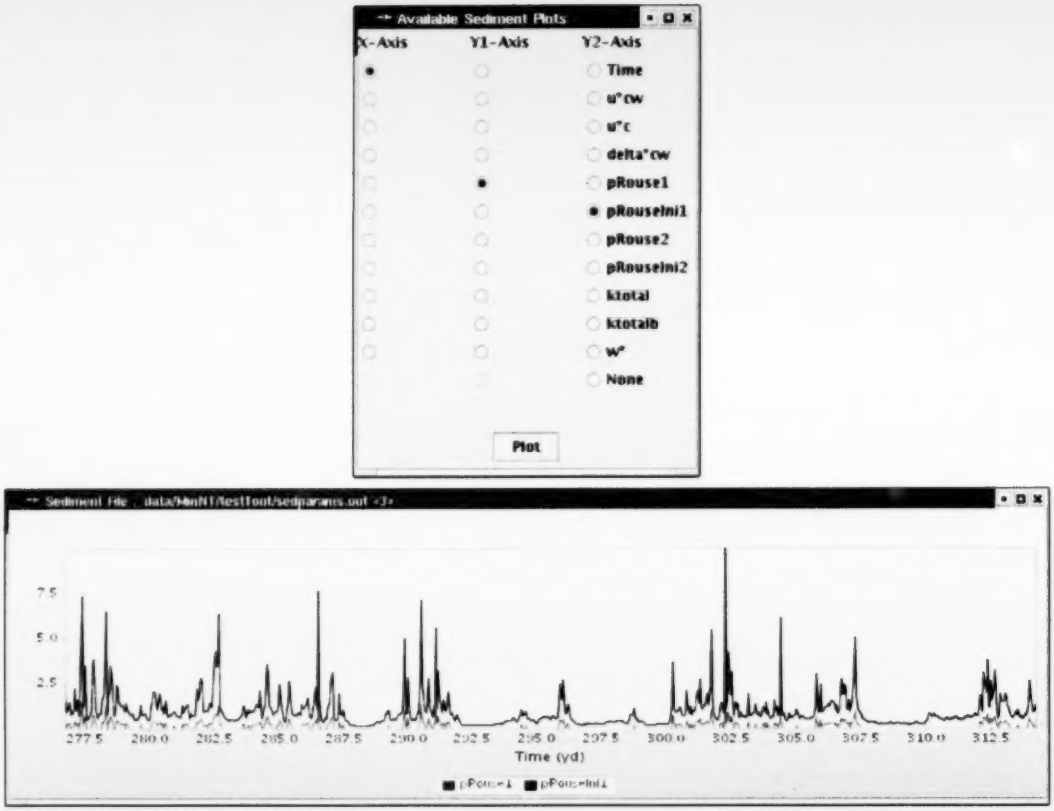

Figure 13: Sediment output plot selection window and resulting plot of Rouse number.

6.2.2 Velocity file (Line 19-20, GUI: R1-R2)

This file can contain the u and v components of velocity at each height above the bottom (those at which data are provided as well as calculated values in the near-bottom log-layer). The columns are time (hours), height (m), u ($\mathrm{m\,s^{-1}}$), and v ($\mathrm{m\,s^{-1}}$). The vertical profiles at chosen times are appended. The module that generates this file is `velout`.

6.2.3 Statistics file (Line 21-23, GUI: S1-S5)

This file summarizes the overall statistical properties of the sediment patch. Appendix H.2 contains a sample. Figure 14 contains the GUI option screen for plotting various columns of the statistics file, along with a plot of mean height. The columns of the statistics file are: time, $\overline{X}$, $\overline{Y}$, $\overline{Z}$, σ^2_{max}, σ^2_{min}, θ, $c1$, $c2$, where time is in year days, ($\overline{X}$, $\overline{Y}$, $\overline{Z}$) is the center of mass of the sediment in meters, σ^2_{max} and σ^2_{min} are the variances of the major and minor axis, θ is the angle that the axis of maximum variance makes with the x-axis (positive = counter clockwise), $c1$ is the depth-integrated or 2-d concentration ($\mathrm{g\,m^{-2}}$)

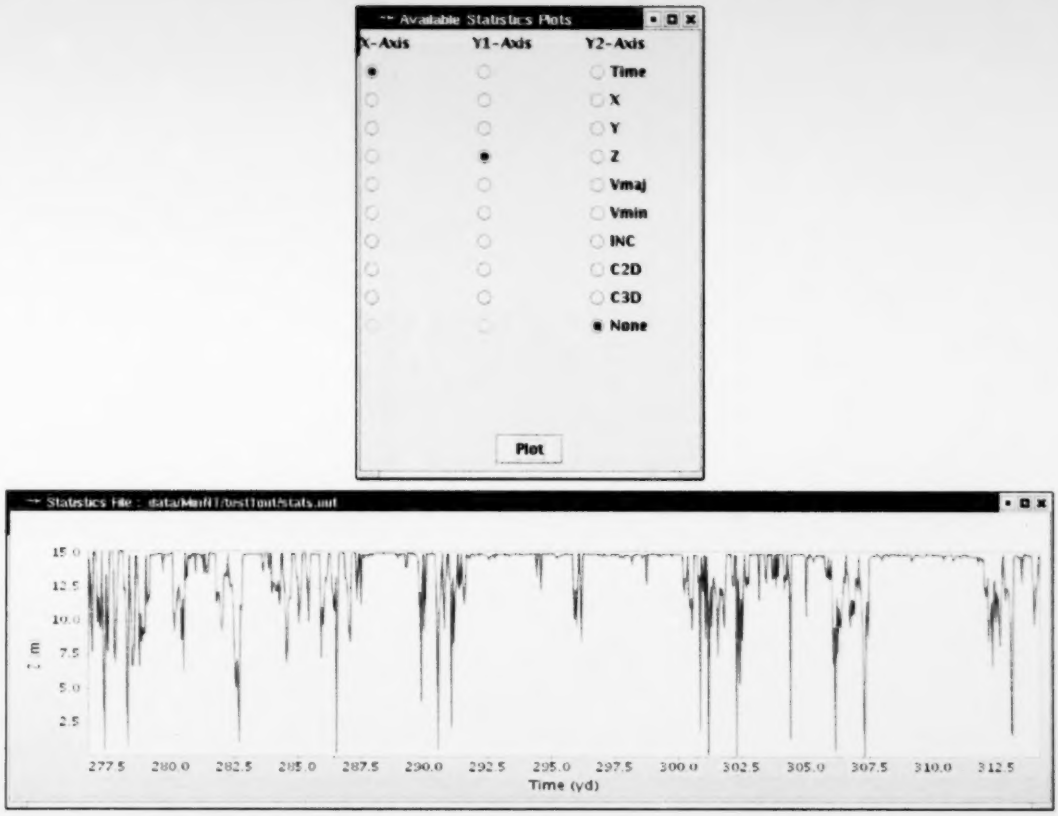

Figure 14: Statistics output plot selection window and resulting plot of mean sediment height.

at the center of mass, and $c2$ is the 3-d concentration ($\mathrm{g\,m^{-3}}$) at the center of mass for the user defined cylinder radius and vertical extent. The module that generates this file is `statout2`.

6.2.4 Packet positions file (Line 24-25, GUI: T1-T2)

This file contains the 3-D location of each packet at the time step specified by the user. The first line of this output file is a header. Subsequently at each time step, `bblt` prints a line containing the time. The next N lines contain the x, y, and z positions of each packet (all in meters). The packet positions are a basic `bblt` output that is used to generate all other outputs. This file can be very large and is rarely useful. The module that generates this file is `packout`.

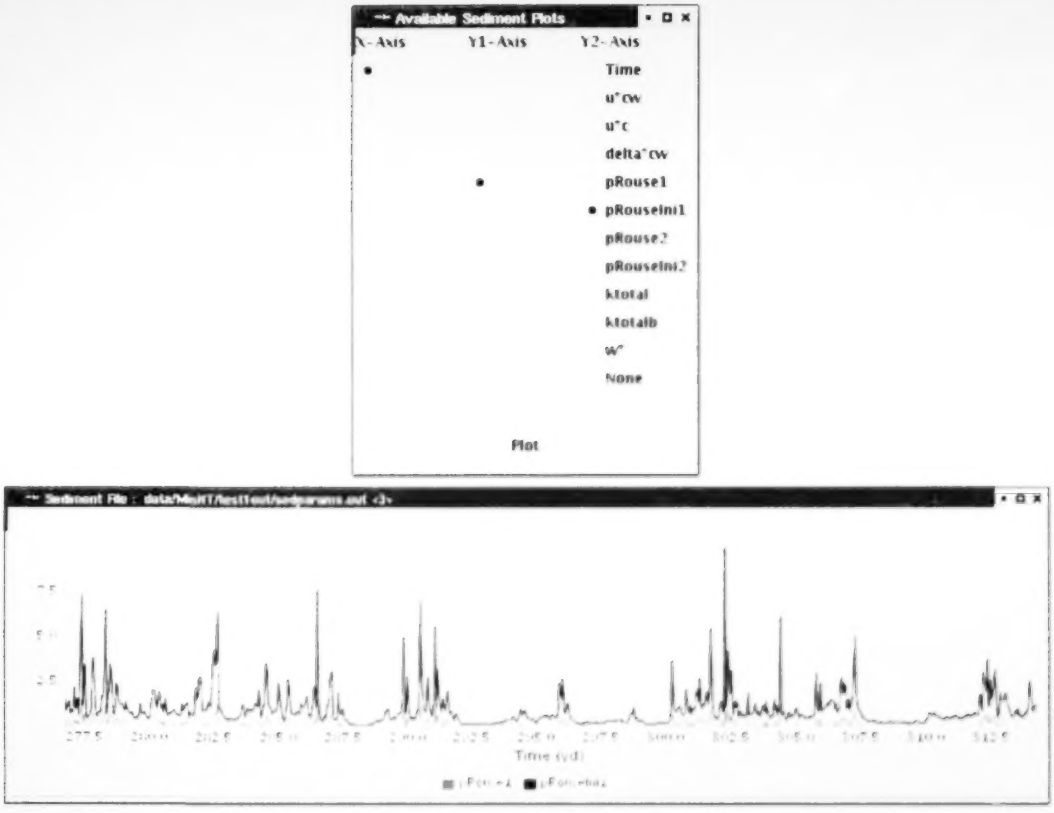

Figure 13: Sediment output plot selection window and resulting plot of Rouse number.

6.2.2 Velocity file (Line 19-20, GUI: R1-R2)

This file can contain the u and v components of velocity at each height above the bottom (those at which data are provided as well as calculated values in the near-bottom log-layer). The columns are time (hours), height (m), u ($\mathrm{m\,s^{-1}}$), and v ($\mathrm{m\,s^{-1}}$). The vertical profiles at chosen times are appended. The module that generates this file is `velout`.

6.2.3 Statistics file (Line 21-23, GUI: S1-S5)

This file summarizes the overall statistical properties of the sediment patch. Appendix H.2 contains a sample. Figure 14 contains the GUI option screen for plotting various columns of the statistics file, along with a plot of mean height. The columns of the statistics file are: time, $\overline{X}$, $\overline{Y}$, $\overline{Z}$, σ^2_{max}, σ^2_{min}, θ, $c1$, $c2$, where time is in year days, ($\overline{X}$, $\overline{Y}$, $\overline{Z}$) is the center of mass of the sediment in meters, σ^2_{max} and σ^2_{min} are the variances of the major and minor axis, θ is the angle that the axis of maximum variance makes with the x-axis (positive = counter clockwise), $c1$ is the depth-integrated or 2-d concentration ($\mathrm{g\,m^{-2}}$)

Figure 14: Statistics output plot selection window and resulting plot of mean sediment height.

at the center of mass, and $c2$ is the 3-d concentration ($\mathrm{g\,m^{-3}}$) at the center of mass for the user defined cylinder radius and vertical extent. The module that generates this file is `statout2`.

6.2.4 Packet positions file (Line 24-25, GUI: T1-T2)

This file contains the 3-D location of each packet at the time step specified by the user. The first line of this output file is a header. Subsequently at each time step, `bblt` prints a line containing the time. The next N lines contain the x, y, and z positions of each packet (all in meters). The packet positions are a basic `bblt` output that is used to generate all other outputs. This file can be very large and is rarely useful. The module that generates this file is `packout`.

Figure 15: Concentration output plot selection window and resulting time series at a particular position.

6.2.5 Concentration time series file (Line 26-29, GUI: U1-U3)

This file contains the time series of concentration at locations specified by the user. An example is given in Appendix H.3. Figure 15 shows the window of the GUI where the information about concentration position and sampling volume is entered. This window also contains buttons for plotting the concentration time series, an example of which can be seen in the same figure.

The concentration file format is as follows. After two header lines, `bblt` lists the positions of the time series locations in x, y, and z. After a blank line follow columns of numbers representing the concentrations in $\mathrm{g\,m^{-3}}$ (or $\mathrm{mg\,L^{-1}}$). The first column is time in yeardays, and all others are concentrations. There are as many columns as user-specified locations.

The module that generates this file is `controut`.

6.2.6 Concentration map file (Line 30-32, GUI: V1-V10)

The concentration map (or snapshot) file is quite long and is not shown. Figure 16 contains a single snapshot of the concentration map for North Triumph. The GUI can display the maps as intensity colour plots at different times and has a limited animation capability.

The basic structure of the concentration map file is as follows. The first line is a header line. The second line contains the total number of timesteps at which the snapshots are given. The third line is the number of grid points in the x-direction (31 for the North Triumph example). The next lines are the x-coordinates of the grid points written out 1 per line. The next line is the number of grid points in the y-direction (for the North Triumph example) The next lines are the y-coordinates of the grid points written out 1 per line. That completes the definition of the grid on which the concentrations are computed. The rest of the file is the data. Each data block consists of a time stamp followed by the 3D concentrations ($\mathrm{mg\,L^{-1}}$) and 2D concentrations ($\mathrm{g\,m^{-2}}$) below at each point on the grid. Each data item is written 1 per line, and the grid is traversed in the

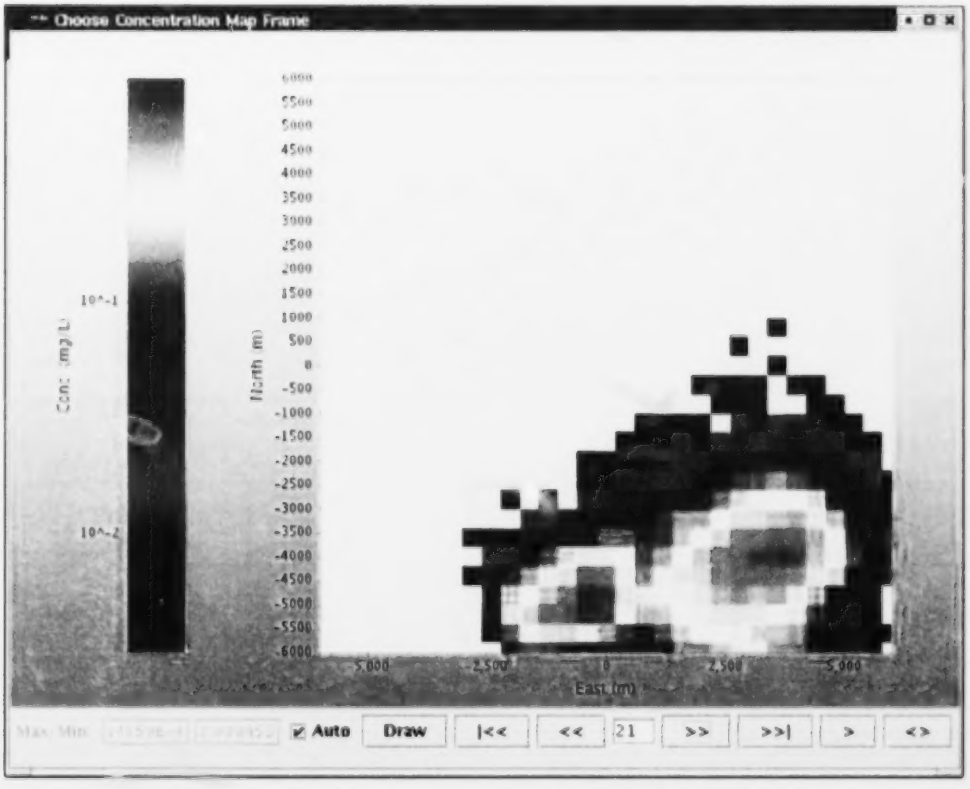

Figure 16: A snapshot of the concentration map.

6.2.6 Concentration map file (Line 30-32, GUI: V1-V10)

The concentration map (or snapshot) file is quite long and is not shown. Figure 16 contains a single snapshot of the concentration map for North Triumph. The GUI can display the maps as intensity colour plots at different times and has a limited animation capability.

The basic structure of the concentration map file is as follows. The first line is a header line. The second line contains the total number of timesteps at which the snapshots are given. The third line is the number of grid points in the x-direction (31 for the North Triumph example). The next lines are the x-coordinates of the grid points written out 1 per line. The next line is the number of grid points in the y-direction (for the North Triumph example) The next lines are the y-coordinates of the grid points written out 1 per line. That completes the definition of the grid on which the concentrations are computed. The rest of the file is the data. Each data block consists of a time stamp followed by the 3D concentrations (mg/L) and 2D concentrations (g/m^2) below at each point on the grid. Each data item is written 1 per line and the grid is traversed in the

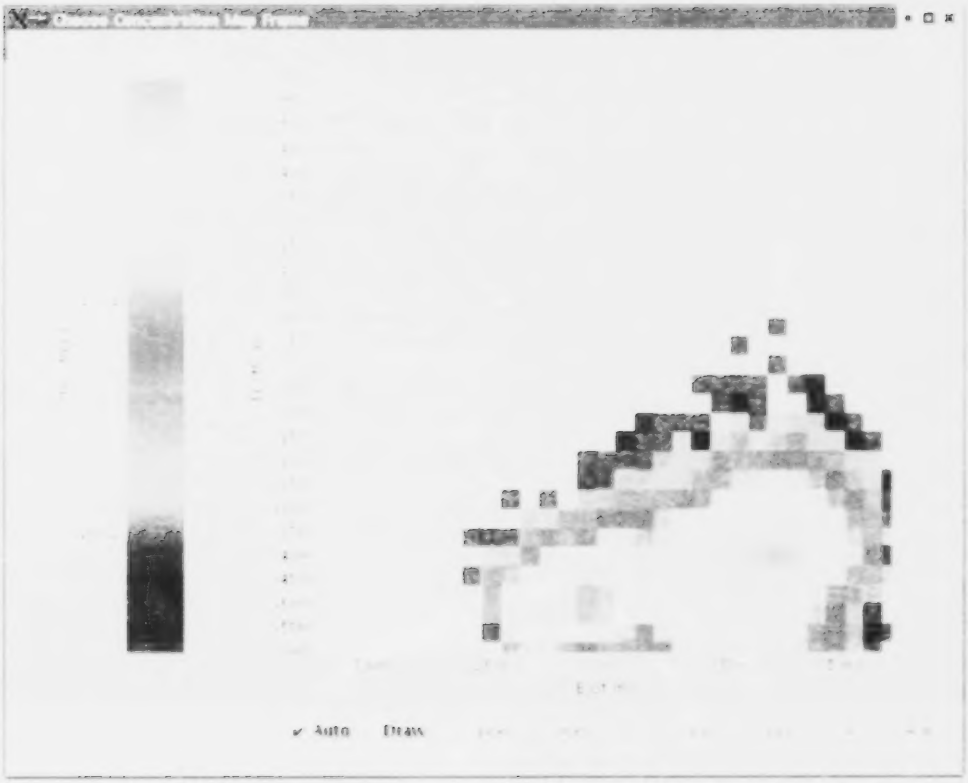

Figure 16: A snapshot of the concentration map.

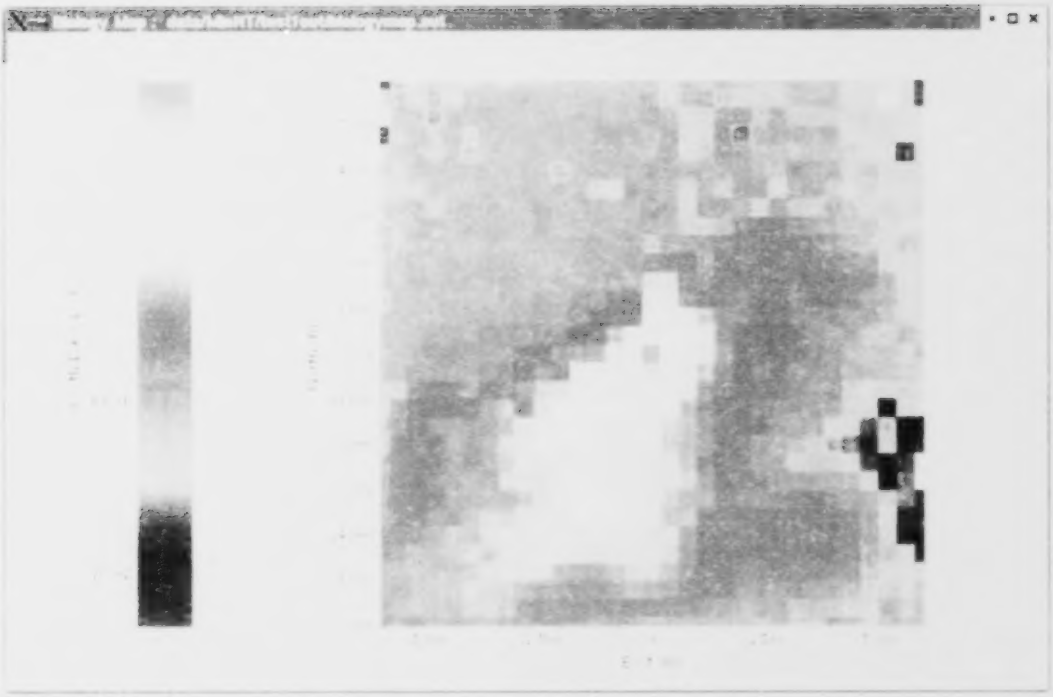

Figure 17: A sample biological impacts map

x-direction (row-wise).

The module that generates this file is `contrmaout`.

6.2.7 Biological impacts file (Line 33-35, GUI: W1-W4)

This file contains the biological impacts at stations defined for the concentration output. Appendix H.4 contains a sample output. The columns of the file are as follows: station number, x, y, and z coordinates of the station, percent of growth days lost, and finally the total growth days lost over the whole simulation.

6.2.8 Biological impacts map file (Line 36-38, GUI: Z1-Z4)

This file contains the biological impacts over the grid defined for the concentration map. The format of the file is a matrix with dimensions matching the grid defined for the concentration map file. Figure 17 shows the biological impacts map for the North Triumph simulation.

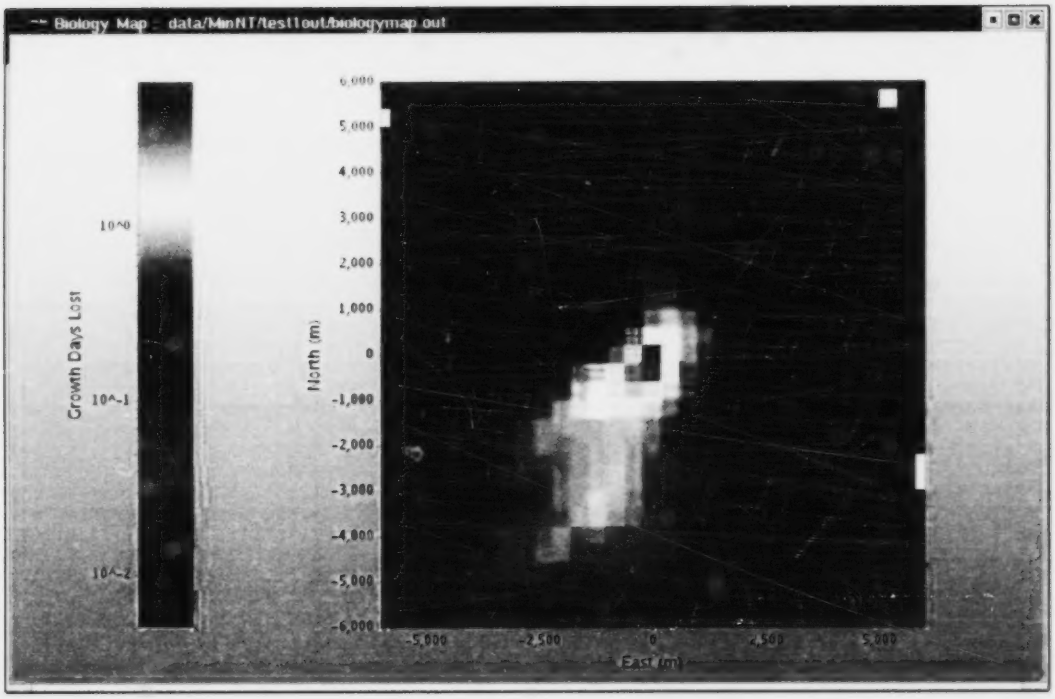

Figure 17: A sample biological impacts map.

x-direction (row-wise).

The module that generates this file is `contrmaout`.

6.2.7 Biological impacts file (Line 33-35, GUI: W1-W4)

This file contains the biological impacts at stations defined for the concentration output. Appendix H.4 contains a sample output. The columns of the file are as follows: station number, x, y, and z coordinates of the station, percent of growth days lost and finally the total growth days lost over the whole simulation.

6.2.8 Biological impacts map file (Line 36-38, GUI: Z1-Z4)

This file contains the biological impacts over the grid defined for the concentration map. The format of the file is a matrix with dimensions matching the grid defined for the concentration map file. Figure 17 shows the biological impacts map for the North Triumph simulation.

7 Final Comments

`bblt v7.0` is a tool for predicting the transport and dispersion of suspended particulate drill waste in the benthic boundary layer. The model combines information on the currents, the settling velocity, the bottom stress, the sediment concentration profile and the discharge scenario to generate estimates of drift, dispersion and concentration. The new graphical user interface and biological impacts module should make the model accessible to a wide range of potential users. At the time of publication, `bblt v7.0` could be downloaded from `www.mar.dfo-mpo.gc.ca/science/ocean/coastal_hydrodynamics/WEBbbltgui/bbltgui.html`

`bblt v7.0` provides much greater flexibility in specifying the bottom stress and the settling velocity. The new user may find the array of choices daunting. The approach taken in the example, whereby the bottom stress includes the combined effects of waves and currents as computed by SEDTRANS96 and the settling velocity is stress dependent, represents our current approach.

The specification of the settling velocity will always be problematic. The best choice of settling velocity depends strongly on what material is being modelled. During the development of `bblt` the emphasis has shifted from whole mud to bentonite plus barite to barite. The focus on barite has emerged because of its greater potential for impact and because of its high density (and resulting high single grain settling velocity). This focus on barite has reduced the emphasis on flocculation dynamics since single grains do not breakup under high stress (and thus the suggestion that $w_1 = w_2$ when modelling the transport of barite).

When simulating realistic discharge scenarios, the discharge time series is of great importance. The uncertainties in the simulated concentrations are directly proportional to the uncertainty in the discharge.

The next focus of the research is on the partitioning of the barite between the suspended fraction and the fraction that gets incorporated into the sea floor. This will directly affect how much material is available for transport and provide information on the potential for barite to remain in the vicinity of the discharge platform.

In closing, a successful run of `bblt v7.0` results in the phrase 'Clean Exit' being written to standard output and the echo file. If this phrase is not written out then `bblt v7.0` did not run correctly.

Acknowledgements

We thank John Loder for ongoing encouragement and support in the development and application of `bblt`, Elizabeth Gonzalez and Yingshuo Shen for contributions to model implementation. We also thank Tim Milligan and Kee Muschenheim for advice on flocculation and settling velocity. This work was supported by the (Canadian) Federal Program for Energy Research and Development.

References

Anderson, C., 2001. Seabed shear stress estimates at the Cohasset and Hibernia oil production sites. Can. Data Rep. Hydrogr. Ocean Sci. 216: viii+54 pp.

Boudreau, P. R., et al., 1999. The possible environmental impacts of petroleum exploration activities on the Georges Bank ecosystem. Can. Tech. Rep. Fish. Aquatic Sci. 2259: vi+106 pp.

Cranford, P. J., 1995. Relationship between food quantity and quality and absorption efficiency in sea scallops *placopecten magellanicus* (Gmelin). J. Exp. Mar. Biol. Ecol. 189, 123–142.

Cranford, P. J., Gordon, D. C., 1992. The influence of dilute clay suspensions on sea scallop (*placopecten magellanicus*) feeding activity and tissue growth. Netherlands J. Sea Res. 30, 107–120.

Cranford, P. J., Gordon, Jr., D. C., Hannah, C. G., Loder, J. W., Milligan, T. G., Muschenheim, D. K., Shen, Y., 2003. Modelling potential effects of petroleum exploration drilling on northeastern georges bank scallop stocks. Ecological Modelling 166, 19–39.

Cranford, P. J., Gordon, Jr., D. C., Lee, K., Armsworthy, S. L., Tremblay, G. H., 1999. Chronic toxicity and physical disturbance effects of water- and oil-based drilling fluids and some major constituents on adult sea scallops (*placopecten magellanicus*). Mar. Env. Res. 48, 225–256.

Csanady, G. T., 1973. Turbulent Diffusion in the Environment. D. Reidel Publishing Company.

Dyer, K. R., 1986. Coastal and Estuarine Sediment Dynamics. Wiley and Sons.

Fischer, H. B., List, E. J., Koh, R. C. Y., Imberger, J., Brooks, N. H., 1979. Mixing in Inland and Coastal Waters. Academic Press.

Gordon, Jr., D. C., Cranford, P. J., Hannah, C. G., Loder, J. W., Milligan, T. G., Muschenheim, D. K., Shen, Y., 2000. Modelling the transport and effects on scallops of water-based drilling mud from potential hydrocarbon exploration on Georges Bank. Can. Tech. Rep. Fish. Aquat. Sci. 2317: 115 pp.

Grant, W. D., Madsen, O. S., 1986. The continental shelf bottom boundary layer. Annual Review of Fluid Mechanics 18, 265–305.

Hannah, C. G., Drozdowski, A., Muschenheim, D. K., Loder, J., Belford, S., MacNeil, M., 2003. Evaluation of drilling mud dispersion models at SOEI Tier I sites: Part 1 North Triumph, Fall 1999. Can. Tech. Rep. Hydrogr. Ocean Sci. 232: v+51 pp.

Hannah, C. G., Loder, J. W., Shen, Y., 1996. Shear dispersion in the benthic boundary layer. In: Spaulding, M. L., Cheng, R. T. (Eds.), Estuarine and Coastal Modeling: Proceedings of the 4th International Conference. ASCE, pp. 454–465.

Hannah, C. G., Shen, Y., Loder, J. W., Muschenheim, D. K., 1995. `bblt`: Formulation and exploratory applications of a benthic boundary layer transport model. Can. Tech. Rep. Hydrogr. Ocean Sci. 166: vi + 52 pp.

Hannah, C. G., Xu, Z., Shen, Y., Loder, J. W., 1998. Models for suspended sediment dispersion and drift. In: Estuarine and Coastal Modeling: Proceedings of the 5th International Conference. ASCE, pp. 708–722.

Hill, P. S., Milligan, T. G., Geyer, W. R., 2000. Controls on effective settling velocity of suspended sediment in the Eel River flood plume. Cont. Shelf Res. 20, 2095–2111.

Hill, P. S., Syvitski, J. P., Cowan, E. A., Powell, R. D., 1998. In situ observations of floc settling velocities in Glacier Bay, Alaska. Marine Geology 145, 85–94.

Hill, P. S., Voulgaris, G., Trowbridge, J. H., 2001. Controls on floc size in a continental shelf bottom boundary layer. J. Geophys. Res. 106, 9543–9549.

L'Ecuyer, P., Cote, S., 1991. Implementing a random number package with splitting facilities. ACM Transactions on Mathematical Software 17, 98–111.

Li, M. Z., Amos, C. L., 2001. SEDTRANS96: The upgraded and better calibrated sediment-transport model for continental shelves. Comput. Geosci. 27, 619–645.

Loder, J., Hannah, C. G., Shen, Y., Gonzalez, E. A., Xu, Z., 1998. Suspended sediment drift and dispersion on Georges Bank, unpublished manuscript with 188 pages. Many of the results were reported in Gordon et al. (2000). Available from `http://www.mar.dfo-mpo.gc.ca/science/ocean/coastal_hydrodynamics/bibliography.html`.

Lynch, D. R., Ip, J. T. C., Naimie, C. E., Werner, F. E., 1996. Comprehensive coastal circulation model with application to the Gulf of Maine. Cont. Shelf Res. 16, 875–906.

Milligan, T. G., Hill, P. S., 1998. A laboratory assessment of the relative importance of turbulence, particle composition, and concentration in limiting maximal floc size and settling behaviour. J. Sea Research 39, 227–241.

Muschenheim, D. K., Milligan, T. G., 1996. Flocculation and accumulation of fine drilling waste particles on the Scotian Shelf. Mar. Pollut. Bull. 32, 740–745.

Muschenheim, D. K., Milligan, T. G., Gordon, D. C., 1995. New technology and suggested methodologies for monitoring particulate wastes discharged from offshore oil and gas drilling platforms and their effects on benthic boundary layer environment. Can. Tech. Rep. Fish. Aquat. Sci. 2049: x + 55 pp.

Naimie, C. E., 1996. Georges Bank residual circulation during weak and strong stratification periods - Prognostic numerical model results. J. Geophys. Res. 101, 6469–6486.

Preisendorfer, R. W., 1988. Principal Component Analysis in Meteorology and Oceanography. Elsevier.

Rouse, H., 1937. Modern concepts of the mechanics of turbulence. Trans. Am. Soc. Civ. Eng. 102, 463–543.

Sumer, B. M., 1974. Mean velocity and longitudinal dispersion of heavy particles in turbulent open-channel flow. J. Fluid Mech. 65, 11–28.

Taylor, G. I., 1921. Diffusion by continuous movements. Proc. London Math. Soc. A20, 196–211.

Taylor, G. I., 1953. Dispersion of soluble matter in solvent flowing slowly through a pipe. Proc. Royal Soc. London A219, 186–203.

Tedford, T., Drozdowski, A., Hannah, C. G., 2003. Suspended sediment drift and dispersion at Hibernia. Can. Tech. Rep. Hydrogr. Ocean Sci. 227: vi + 57 pp.

Tedford, T., Gonzalez, E., Hannah, C. G., 2001. `bblt` version 3.1 user's manual. Can. Tech. Rep. Hydrogr. Ocean Sci. 213: v + 48 pp.

van Rijn, L. C., 1993. Principles of Sediment Transport in Rivers, Estuaries and Coastal Seas. Aqua Publications, Amsterdam.

Xu, Z., Hannah, C. G., Loder, J. W., 2000. A 3d shear dispersion model applied to Georges Bank. In: Spaulding, M. L. (Ed.), Estuarine and Coastal Modelling: Proceedings of the 6th International Conference. ASCE, pp. 294–309.

A List of Symbols

List of symbols found in the text.
Table 2 contains additional symbols which are `bblt` inputs.

t	time
z	vertical coordinate, $z = 0$ at the sea floor and positive upward
z_0	bottom of log-layer
$\mathbf{x}$	horizontal position coordinate
$\mathbf{u}$,	the current velocity
$\mathbf{u_b}$	the observed near bottom current
τ_b	general bottom stress
$u_* = \sqrt{\tau_b/\rho}$	general friction (shear) velocity
w_s	settling velocity
h	maximum height of suspended sediment and effective water depth (a.k.a h_{max})
a	sediment reference height (a.k.a h_{ref})
$p = \beta w_s/\kappa u_*$	Rouse number
p_1, p_2	Rouse numbers for the current-wave and current layers
p_{1in}, p_{2in}	Rouse numbers used internally by `bblt` (Table 3)
β	Rouse number scaling factor
$\epsilon(z)$	the mixing coefficient at height z above the sea floor
$c(z)$	the Rouse vertical concentration profile
c_a	the reference concentration at the reference height $z = a$
c_δ	the concentration at height $z = \delta$
$F(z)$	fraction of total mass in the interval $[a, z]$
$H(p, v)$	intermediate expression used in solving $F(z)$
η	intermediate expression used in calculating $F(z)$
N_b	Number of packets having experienced breakup at least once.
n	packet label, $n = 1, 2, \ldots, N$
α_n	rank which maps $F(z) \rightarrow Z_n$
$X_n(t)$, $Y_n(t)$	horizontal position of the n^{th} packet at time t
$Z_n(t)$	vertical position of the n^{th} packet at time t
q	an integer, see algorithm outline (Section 4)
γ	the number of vertical shuffles performed at each Δt_a
$C(t)$	the near-bottom concentration at time t
PGI	the potential growth inhibition
N_t	the total number of timesteps for the period considered
t_i	the time at timestep i
$R(t)$	the growth reduction index at time t
ω	angular frequency
$\overline{X}(t), \overline{Y}(t), \overline{Z}(t)$	the center of mass of the cloud of packets at time t
U, V	the time rate of change of the horizontal center of mass
ζ	the covariance matrix

$\sigma_{xx}^2, \sigma_{yy}^2, \sigma_{xy}^2$	elements of the covariance matrix
$\sigma_{max}^2, \sigma_{min}^2$	major and minor axis components of the covariance matrix
θ	the angle that the axis of maximum variance makes with the x-axis (positive = counter clockwise)
r	radius of sampling cylinder
A	sampling area
z_1, z_2	vertical extent of sampling cylinder
$C_{\min} = \frac{m}{A(z_2 - z_1)}$	the minimum resolvable concentration
u_{*crit}	critical friction for fraction of sediment suspension
ξ	vertical coordinate used in the log-layer calculation (Appendix B)
ξ_0	roughness height used in log-layer calculation
ξ_b	the height above seafloor of the bottom node
u_b	the current speed at the bottom node
ρ	water density
ρ_0	reference density
C_d	drag coefficient
T_L	the Lagrangian time scale
K_{max}, K_{min}	horizontal diffusivities along the major and minor axes
$K = \sqrt{K_{max} K_{min}}$	the effective horizontal diffusivity
K_0	the horizontal dispersion due to steady flow
$< U^2 >$	the mean square velocity deviation
$< \cdot >$	the ensemble average
$T_c = h^2/D$	vertical mixing time scale
T	period of oscillation for rotary currents
$T' = T/T_c$	normalized period of oscillation
$\bar{z}$	the vertical center of mass of the sediment
z_s	a vertical scale height
M_2	the semidiurnal tidal period ($\approx$ 12.4hr)
Φ	scaling factor for vertical mixing time scale

B Logarithmic Sublayer

The implementation of the logarithmic sublayer follows the formalism developed for the finite-element circulation model QUODDY (Naimie, 1996; Lynch et al., 1996), which was used to generate the 3-d circulation fields for spatial `bblt` (Xu et al., 2000). It is a reasonable representation for use with observed currents from the bottom few meters. Understanding the representation of the logarithmic sublayer is important for `bblt` because most of the velocity shear in tidal flows is near the bottom, and it is this velocity shear which generates the dispersion in `bblt`.

Here we describe the details of the logarithmic sublayer implementation, using for illustrative purposes the simplified case of the instantaneous near-bottom flow $\mathbf{u_b}$ directed in the x-direction (or the x-axis rotated to the direction of $\mathbf{u_b}$).

QUODDY does not resolve the entire bottom boundary layer; rather, the bottom of the computational domain is assumed to be in the constant stress layer (log-layer) and displaced a small distance above the ocean bottom. Closure is obtained via a quadratic stress law:

$$\frac{|\tau_\mathbf{b}|}{\rho_0} = u_*^2 = C_d|\mathbf{u}_b|^2 \tag{28}$$

where $\tau_\mathbf{b}$ is the bottom stress, ρ_0 is the reference density, u_* is the friction velocity, C_d is the drag coefficient and $\mathbf{u}_b$ is the velocity at the bottom of the model. We deal with the inconsistency between (28) and (1) later.

Let ξ be the distance above the seafloor, $u(\xi)$ the x-component of velocity, ξ_b the height of the bottom node above the seafloor and $u_b = u(\xi_b)$. The logarithmic profile is

$$u(\xi) = \frac{u_*}{\kappa}\ln(\xi/\xi_0) \tag{29}$$

where ξ_0 is the roughness height, and κ (= 0.4) the von Karman constant. The relationship between ξ_b, ξ_0 and C_d (found by substituting the velocity profile into the stress law) is

$$\xi_0 = \xi_b e^{-\kappa/\sqrt{C_d}} \tag{30}$$

In the present QUODDY solutions, $\xi_b = 1$ m and $C_d = 0.005$ which yields $\xi_0 = 0.003495$ m. Notice that ξ_0 is the height at which the velocity goes to zero, and could be interpreted to mark the transition to the viscous sublayer where horizontal velocities are assumed vanishingly small.

From the point of view of `bblt`, u_b is known so the velocity profile is computed using

$$u(\xi) = u_b\frac{\sqrt{C_d}}{\kappa}\ln(\xi/\xi_0) \quad \text{for } h_{ref} < \xi < \xi_b \tag{31}$$

which is obtained by substituting the stress law into the velocity profile. We also require $\xi_0 < h_{ref}$. With this relation, there is no rotation with height of the velocity in the

logarithmic sublayer so that, in cases where ξ_b is more than a few meters, the profile is only a crude approximation to the bottom Ekman layer.

The logarithmic sublayer presented is self-consistent. What happens if we adjust some of the relationships? In particular, in some cases we want to use a general stress law such as (1) to include additional stresses due to unmodelled velocity components or wave effects. For example, calculations of enhanced stress due to waves and wave-current interactions indicate that, for the water depths of 20-100 m, bottom stress values can be 50–100% larger than those computed from a stress law like (28) (Anderson, 2001). However, the user may still need to take u_b and ξ_b from the 3-d model profile or moored measurements (to focus on velocity changes within the sublayer and the effects of the stress changes on sediment suspension). Under these conditions the velocity profile in the logarithmic sublayer can be written as

$$u(\xi) = u_b + \frac{u_*}{\kappa} \ln(\xi/\xi_b) \tag{32}$$

where $\xi \leq \xi_b$. The friction velocity u_* can now be freely specified (i.e. it is not constrained by (28)).

The consequences of such an adjustment are as follows. Specifying u_* greater than that implied by (28) has the effect of increasing the effective ξ_0, while decreasing u_* decreases ξ_0. In fact, factor of two changes in u_* imply order of magnitude changes in ξ_0. It is easy to generate cases where $\xi_0 > h_{ref}$ for reasonable values of h_{ref}. For $\xi_0 > h_{ref}$ the velocities $u(\xi)$ for $\xi < h_{ref}$ are the opposite sign of u_b. On the other hand, for $\xi_0 \ll h_{ref}$ most of the velocity shear occurs in the region $\xi < h_{ref}$ and there is very little shear dispersion near the bottom.

We have adopted the following procedure in order to avoid having changes in the stress law (1) (which is intended to control the vertical extent of the concentration profile) change the dynamical consistency of the logarithmic sublayer:

- The roughness height $\xi_0 = 0.003495$ m is fixed.
- The height above the bottom of the near-bottom current meter, ξ_b, is taken as specified by the user.
- The drag coefficient C_d is calculated from

$$C_d = (\kappa / \ln(\xi_b/\xi_0))^2 \tag{33}$$

  For $\xi_b = 1$ m $C_d = 0.005$, and for $\xi_b = 3$ m $C_d = 0.0035$.

- The velocities in the sublayer are calculated according to (31).

The velocity profile is discretized at user-specified levels ξ_s with $s = 1, N_{sl}$, and linear interpolation is used to estimate the velocity between these levels (in an identical manner

to the specified velocities above the sublayer). If the user specifies $N_{sl} = 2$, then a linear sublayer is created.

Within `bblt` the calculation of the parameters for the logarithmic sublayer are independent of the calculation of u_*. This is consistent with our approach that the velocity profiles are specified and not changed by sediment processes. However, we have used the relation (33) to calculate the drag coefficient to use with the observed currents where the height above the bottom can range from 3 to 14 m.

The logarithmic sublayer has the feature that the velocity at the reference height is not zero, whereas it was zero in the linear sublayer in `bblt` v1. The velocity at the reference height is

$$u(h_{ref})/u_b = 1 - \ln h_{ref}/\ln \xi_0 \quad . \tag{34}$$

For the typical values of ξ_0 and h_{ref} ($\xi_0 = 0.003495$ m, $h_{ref} = 0.0035$ m) the velocity ratio $u(h_{ref})/u_b = 2.5 \times 10^{-4}$ and the velocity experienced by packets near the bottom is very small. Notice however that for $h_{ref} = 0.01$ m (a reasonable value and the one used in Hannah et al. 1995, 1996, 1998), $u(h_{ref})/u_b = 0.19$ which is quite large and indicates that most of the near bottom shear occurs for $\xi < h_{ref}$.

Appendix G.1 gives an example of the log-layer input file used for the North Triumph sample run.

C SEDTRANS96

SEDTRANS96 (Li and Amos, 2001) calculates a friction velocity associated with grain roughness (skin friction) and a friction velocity associated with the flow separation on bed-forms (bed friction). It utilizes the following inputs at every time step: water depth, mean current velocity and its direction, height of current measurement above the sea bed, significant wave height, wave period, wave propagation direction, median sediment grain size (diameter) and an initial ripple height and wavelength. Following the approach of Grant and Madsen (1986), the friction velocity is decomposed into components due to currents only, waves only and the combined effects of waves and currents. Tedford et al. (2003) provide a discussion of the different types of friction velocity. An integral part of the SEDTRANS96 procedure, is the joint calculation of friction velocity and bed-form types, ripple height and ripple wavelength.

The SEDTRANS96 software converts the currents at the observed height to equivalent currents at 1 mab as part of the stress calculation. The conversion is an iterative procedure which tries to match stress and bed-forms. Tedford et al. (2003) have analyzed the difference between u_* based on 3 and 1 mab currents. The differences are less than 15.2%, 99.9% of the time for all four of the u_*. These discrepancies are small compared to other uncertainties and are typically ignored. The interaction of `bblt` and SEDTRANS96 is depicted in Figure 18.

An additional intermediate SEDTRANS96 output which is used by `bblt` is the height above bottom of the current-wave boundary, δ.

We have modified SEDTRANS96 so that at each timestep it uses the bedform from the previous timestep as the initial bedform.

The SEDTRANS96 software is available from the lead author (Mike Li; Geological Survey of Canada, Bedford Institute of Oceanography, Dartmouth, Nova Scotia) and from `www.iamg.org/CGEditor/index.htm`

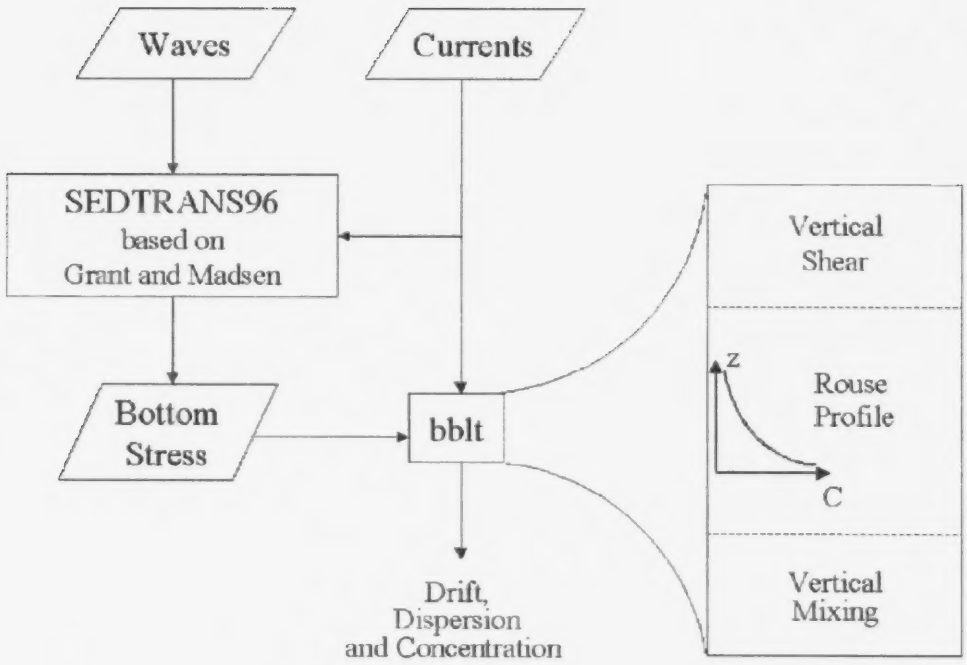

Figure 18: Schematic illustrating interaction between `bblt` and SEDTRANS96. Vertical shear, the Rouse profile and vertical mixing are the primary components of the `bblt` model.

D Validation Through Numerical Experiments

D.1 Steady and Rotary Flow Theory

A useful measure of the strength of the turbulent mixing across the shear (vertical mixing in our case) is the Lagrangian time scale T_L, often interpreted as 'a measure of how long a particle takes to lose memory of its initial velocity' (Fischer et al., 1979) or as the time required for a particle to sample the whole velocity field. Large T_L corresponds to weak mixing and small T_L corresponds to strong mixing.

Consider the case of (horizontally uniform) steady shear flow. For time $t \gg T_L$, the effective horizontal diffusivity K is expected to obey the relation (Taylor 1921, 1953; Fischer et al. 1979)

$$K = < U^2 > T_L \tag{35}$$

where $< U^2 >$ is the mean square velocity deviation (relative to the average flow) experienced by a particle and the ensemble average $< \cdot >$ is the average over a large number of realizations of the flow. This relation is the basis for our interpretation of the results of the numerical experiments.

This section draws heavily on the extensive review and analytical solutions in Fischer et al. (1979, in particular Chapter 4). They derive analytical solutions for shear dispersion in linear shear flow, which we represent as $u(z) = u_0 z$. Their results were presented in the context of horizontal shear but they apply to vertical shear with massless particles (i.e. $w_s = 0$, $p = 0$). In this report, we extend the results to the finite mass case $w_s > 0$, $p > 0$.

For steady flow the horizontal dispersion due to vertical shear is (Eqn 4.22 in Fischer et al. 1979)

$$K_0 = u_0^2 T_c / 120 \tag{36}$$

where $T_c = h^2/D$ is the vertical mixing time scale and a surrogate for T_L, h is the water depth, and D is a vertical diffusion coefficient. The key point is that K_0 is linearly proportional to T_c. Direct comparisons of (36) with solutions from `bblt` requires knowledge of the relationship between T_c and vertical shuffling time scale t_m. We pursue this in the discussion at the end of Section D.2.

For periodic shear flow the mean dispersion is (Eqn 4.55 in Fischer et al. 1979, note that we have dropped the square on the T' inside the summation sign in order to reproduce their Figs. 4.7 and 7.4, and to be consistent with their eqns 4.53 and 4.54)

$$K = \frac{120 K_0}{\pi^4} (T')^2 \sum_{n=1}^{\infty} (2n-1)^{-2} \left\{ \left[\frac{\pi}{2} (2n-1)^2 T' \right]^2 + 1 \right\}^{-1} \tag{37}$$

where $T' = T/T_c$ and T is the period of the oscillation. In the limit of weak mixing ($T/T_c \ll 1$) the time averaged diffusivity $K \to 0$, and for strong mixing ($T/T_c \gg 1$) the diffusivity $K \to K_0/2$. The same limits can be derived from simple physical arguments.

In the limit of no mixing ($T/T_c \to 0$) the particle distribution is sheared out on one phase of the tide and then brought back together on the opposite phase, so that in the mean there is no net dispersion (Fig. 3). Hence $T/T_c \ll 1$ implies $K \to 0$. In tidal time the particle distribution can have maximum variance once or twice a tidal cycle depending on the initial phase of the tidal current (Fig. 3).

For $T/T_c \gg 1$ (strong mixing), the mixing time is much less than the period of the oscillation and the sediment is redistributed vertically faster than it is sheared. The sediment distribution is in quasi-equilibrium with the instantaneous value of the velocity profile and the friction velocity. A factor of $1/2$ comes from averaging $(\sin \omega t)^2$ over a tidal cycle. Hence $T/T_c \gg 1$ implies $K \to K_0/2$.

Under the additional assumption that the `bblt` shuffling time scale t_m is proportional to T_c, the solutions given provide a framework for understanding the dependence of the dispersion rates in `bblt` on t_m, which we treat as a free parameter. Since (36) and (37) are derived under the assumption that $w_s = 0$, the next step is to understand how the dispersion rates will depend on w_s and other parameters which effect the vertical distribution of the sediment.

The velocity deviations experienced by the sediment ($< U^2 >$) are a function of the strength and shape of the shear profile and the vertical scale of the sediment distribution. The vertical scale is determined by the Rouse number, which is a function of both the particle settling velocity and the shear profile (through the shear stress). The relationship between $< U^2 >$ and the vertical scale of the sediment distribution depends on the shape of the shear profile. For example, increasing the Rouse number (and decreasing the vertical scale) will increase $< U^2 >$ if the shear is weaker higher in the water column. However if the shear is stronger higher in the water column then $< U^2 >$ will decrease. This argument is supported by the analytical results of Sumer (1974) who found that for a logarithmic velocity profile (shear decreases with height above the bottom) '... the mean particle velocity decreases and the longitudinal dispersion coefficient of particles increases with fall velocity.'

For linear shear flow we are able to make estimates of the functional dependence of $< U^2 >$ on the strength of the flow and the vertical center of mass of the sediment distribution. The results are independent of the details of the distribution. Assume a linear shear profile, $u(z) = u_0 z/h$. Then a reasonable approximation to the mean square velocity deviations is

$$< U^2 >= \frac{1}{z_s} \int_0^{z_s} (u_0/h)^2 (z - \bar{z})^2 \mathrm{d}z \tag{38}$$

where $\bar{z}$ is the vertical center of mass of the sediment, z_s is the vertical scale height, and

$a = 0$ for convenience. The vertical scale height is loosely defined as the height to which a significant amount of sediment is mixed. In this calculation we have replaced the details of the concentration profile by an estimate of the vertical scale of the profile.

Consider the case where the particles are bottom trapped and the upper boundary is not a factor. Let $z_s = \lambda \bar{z}$, where λ is about 2 or 3,

$$< U^2 >= u_0^2(\bar{z}/h)^2(1 - \lambda + \lambda^2/3) \tag{39}$$

For large Rouse numbers (small $\bar{z}$), K should scale as $\bar{z}^2$.

At the other extreme, when the sediment is uniformly mixed through the water column, the vertical sediment distribution is essentially independent of the sediment properties. Therefore K should be independent of the Rouse number as $p \to 0$ and $\bar{z} \to h/2$.

In summary, previous solutions and existing knowledge of shear dispersion suggest that:

- For steady flow, $K \propto t_m$;
- For periodic flow $\begin{cases} K \to 0 & \text{for weak mixing } (T/t_m \ll 1) \\ K \to K_0/2 & \text{for strong mixing } (T/t_m \gg 1) \end{cases}$
- For linear shear $\begin{cases} K \propto \bar{z}^2 \text{ as } \bar{z} \to a \\ \text{K only weakly dependent on } \bar{z} \text{ as } \bar{z} \to h/2 \end{cases}$

The numerical experiments that follow verify the first two hypothesis, the third is discussed by Hannah et al. (1995).

D.2 Numerical Experiments

In this section we compare the results of some simple numerical experiments using `bblt v7.0` with the analytical results described in Appendix D.1. We use steady flow for an evaluation of the basic model and to explore parameter sensitivities. Then we move to rotary current flow. We close with a discussion of the relationship between our vertical shuffling time scale t_m, shuffling method and the mixing time scale used in the analytical solutions.

The fixed parameter values used in the experiments are listed in Table 4. The packet mass is not pertinent to the experiments and thus not mentioned.

In all cases the velocity profile is linear. The velocity is a maximum at the surface and goes to 0 at the reference depth, $z = a$. There is no bedload transport $u(z \leq a) = 0$. The linear profile is used so that direct comparisons can be made with the analytical solutions.

water depth	$h = 10$ m
reference depth	$a = 0.01$ m
velocity profile	$u(z) = u_0(z - a)/h$
	$u_0 = 0.5$ m s^{-1}
bottom friction	$a_1 = 2.0 \times 10^{-4}$ m s^{-1}
	$a_i = 0.0 \ \forall \ i \neq 1$
near bottom velocity	$u(10)$, the velocity 10 m off the bottom
number of packets	N = 50000, initially at origin
integration time	$t_t = 100$ hr
	$t_t = 400$ hr when $t_m \geq 100$ hr
velocity time step	$\Delta t_U = 1.0$ hr
advection time step	$\Delta t_a = 0.1$ hr
settling velocity	$w_s = 0.004$ m s^{-1}
von Karman constant	$\kappa = 0.4$

Table 4: Parameter values for numerical experiments

The amplitude of the velocity profile, the bottom friction coefficients a_1 and a_2 (Section 3.2) and the particle settling velocity w_s were chosen to generate a Rouse number of 1.0.

The sensitivity of the results to the shuffling time scale t_m, shuffling method and the advective time step Δt_a is investigated.

The horizontal diffusivity is computed as described in Section 3.9. This definition of diffusivity is a depth-integrated view. It addresses the question of how far from the center of mass does the cloud of sediment extend, without regard for whether the sediment is near the bottom or higher in the water column. In regions with weak mean currents and rectilinear tidal currents the depth-integrated view is representative of the near bottom region because all the sediment settles to bottom twice a tidal cycle. In regions with rotary tidal currents the concentration profile may not collapse and the dispersion rate in the near bottom region may not be well represented by the depth-integrated view.

We note that the time history of the sediment concentration at a point is a function of the mean velocity (i.e. the horizontal movement of the center of mass), the diffusivity (i.e. the horizontal dispersion) and the friction velocity. The mean velocity and the diffusivity determine how far afield the sediment moves and the friction velocity determines the vertical distribution of the sediment at the time of interest.

Steady Flow

The purpose of the steady flow experiments is to demonstrate that the results of `bblt v7.0` are consistent with the basic model of shear dispersion presented in Appendix D.1. Here we assume that t_m is linearly proportional to both T_L and T_c and, following the

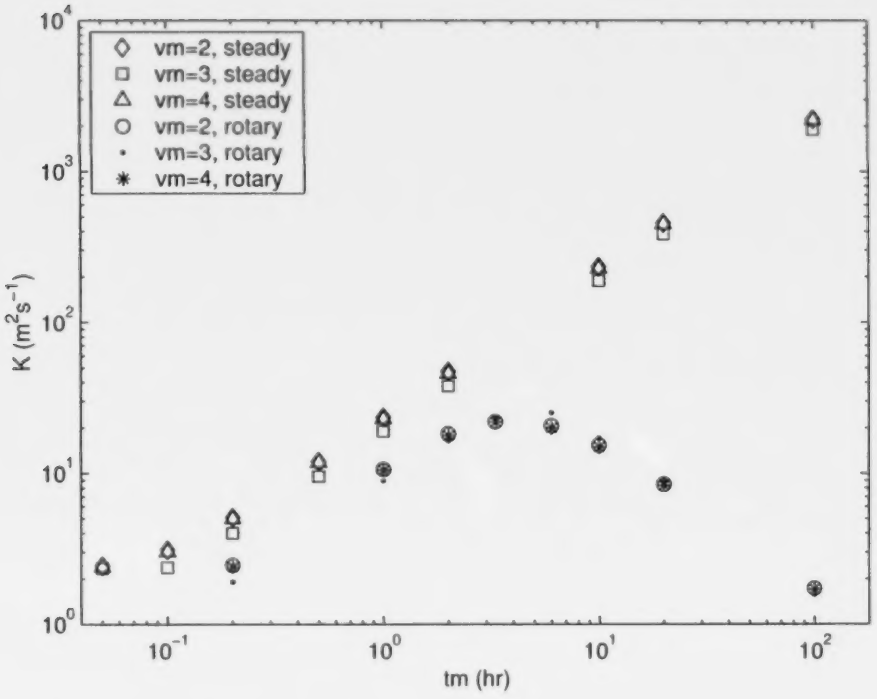

Figure 19: Effective horizontal diffusivity as a function of t_m for steady and rotary shear flow and for various vertical shuffling methods (vm).

form of (35), write

$$K = k < U^2 > t_m \tag{40}$$

where k is a constant. We hold the flow field and the settling velocity constant (thus fixing $< U^2 >$) to demonstrate that $K \propto t_m$. The simulation parameters are listed in Table 4.

The results in Figure 19 show that $K \propto t_m$ over the range $0.1 \leq t_m < 100$ hr. The relationship does not hold for $t_m < \Delta t_a = 0.1$ hr. which is the source of the requirement that $t_m > \Delta t_a$ It is encouraging to note that the 3 different shuffling schemes give very similar results. The constant $k = 22.1, 19.0$ and 21.9 for methods 2, 3 and 4 respectively. The results differ by about 5-10%.

Rotary Flow

Rotary flow adds the effect of time varying current but keeps the magnitude of the current constant. We consider purely periodic flow at the semidiurnal M_2 tidal period, $T = 12.4$ hr. The time dependence of the currents is given by:

$$u(z,t) = u(z) \sin \omega t \tag{41}$$

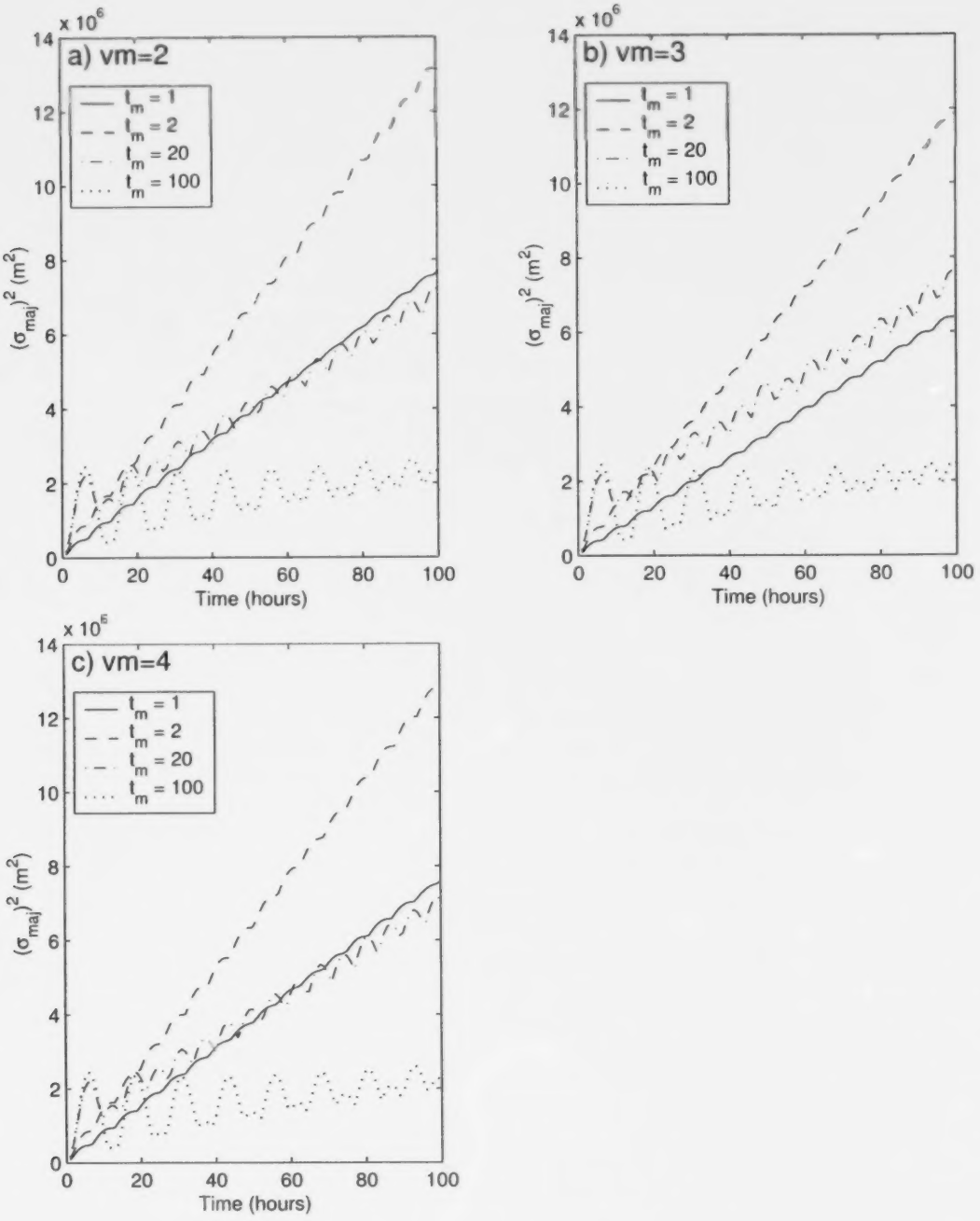

Figure 20: Packet major-axis variance (σ_{maj})as a function of time for rotary flow. Labeled a)-c) are the different vertical shuffling methods (vm). The mixing time scales are t_m = 1, 2, 20, 100 hr. The minor-axis (σ_{min}) plots are similar.

$$v(z,t) \;=\; u(z)\cos\omega t, \tag{42}$$

where $\omega = 2\pi/T = 1.4 \times 10^{-4}$ rad s^{-1}. The basic parameters and $u(z)$ are defined in Table 4.

Figure 20 shows the packet variance due to rotary currents for the different shuffling schemes and various values of t_m. In the case of strong mixing (small t_m) the packet variance shows only a weak modulation at twice the tidal frequency. In the case of weakest mixing (t_m = 100 hr) the packet variance experiences large variations at the tidal frequency and there is a secondary peak growing to match the first peak. The growing second peak indicates that after 8 tidal cycles (100 hrs) the simulation has not reached a statistical equilibrium. This is consistent with the result from the steady case where roughly 2N exchanges were required for complete mixing (i.e. all the packets lose knowledge of their initial conditions). The details of the variance time series would be different for different initial phases of the velocity time series.

The effective horizontal diffusivity as a function of t_m is very similar for the different shuffling schemes (Figure 19). Note that the maximum diffusivity occurs for $t_m \sim 3$ hr or about 1/4 of the tidal period.

In the rotary current case, u_* and $\bar{z}$ are constant while the currents vary. This makes the result directly comparable with the analytical results in Section D.1. Notice that for $t_m < 3$ hr ($\sim T/4$) the diffusivities are about 1/2 the steady values, consistent with the strong mixing case, $T/T_c \gg 1$.

For large t_m the effective horizontal diffusivity goes to zero, consistent with the weak mixing case $T/T_c \gg 1$. As explained in Section 3.1, the packets can experience large shear during a tidal cycle but when averaged over a tidal cycle the effective diffusivity is small. In the limit of no vertical mixing, there is no mean shear dispersion from periodic flow.

Discussion

We have demonstrated that the functional dependence of K on t_m is in reasonable agreement with theory.

In the steady case K is linearly proportional to t_m for $t_m > 2\Delta t_a$ (Figure 19), consistent with (40). Furthermore K does not decrease for $t_m < \Delta t_a/2$, consistent with the packets being completely mixed after 2N exchanges.

Similar results have been obtained for other settling velocities. For a more complete investigation see Hannah et al. (1995). Another result from that paper which we quote here is a demonstration that the velocity of the horizontal center of mass is equal to the value of the velocity profile evaluated at the vertical center of mass. This must be true (by definition) and has been verified by numerical experiments.

For the rotary case, it's important to ask whether the overall magnitude of the shear dispersion is in reasonable agreement with the theory. This requires a relationship between

t_m and T_c (Section D.1). Let $t_m = T_c/\Phi$. In Figure 21 we compare the rotary results with (37) for $\Phi = 1, 5, 10$. Hannah et al. (1995). estimated $\Phi = 5.3$ for shuffling method 2, from a similar analysis. The diffusivities from Fig. 19 have been scaled to correspond with Fig. 7.4 in Fischer et al. (1979): $(T_c/T)K/(K_0/2)$, where $K_0 = \lambda t_m$ and λ is the slope of the steady results in Figure 19. It is clear the $\Phi \sim 4 - 5$ gives good results. The fact that T/T_c appears on both axes means that changes in Φ affect both the amplitude and location of the maximum in the numerical K.

E Sample Input File

The name of the input file below is **NTriumph.bblt** and it can be found in **data/NorthTriumph/** with the distribution. Sections 5 and 6 explain the process involved in creating an input file.

```
data/NorthTriumph/test1out/echo.out
379481019 831796018
900 276.708
1
0.1 4
2
-2
data/NorthTriumph/currents/TS2eUe3_UST2L_1.dat
0.005 0.001 0.0001 0.01
0.4 0.0035
30
0
data/NorthTriumph/currents/NT1-HIGH1Hstep_60K.o1d
data/NorthTriumph/currents/hloglayer2.3m
data/NorthTriumph/currents/TS2eUe3.heights
data/NorthTriumph/currents/TS2eUe3_67m_1.o1d
data/NorthTriumph/currents/TS2eUe3_65m_1.o1d
data/NorthTriumph/currents/TS2eUe3_63m_1.o1d
data/NorthTriumph/currents/TS2eUe3_61m_1.o1d
data/NorthTriumph/currents/TS2eUe3_56m_1.o1d
data/NorthTriumph/currents/TS2eUe3_51m_1.o1d
data/NorthTriumph/currents/TS2eUe3_41m_1.o1d
data/NorthTriumph/currents/TS2eUe3_31m_1.o1d
1.0
data/NorthTriumph/test1out/sedparams.out
0.0
1.0
data/NorthTriumph/test1out/stats.out
0.0035 0.1035 250
0.0
1.0
data/NorthTriumph/test1out/cnstr.out
38
```

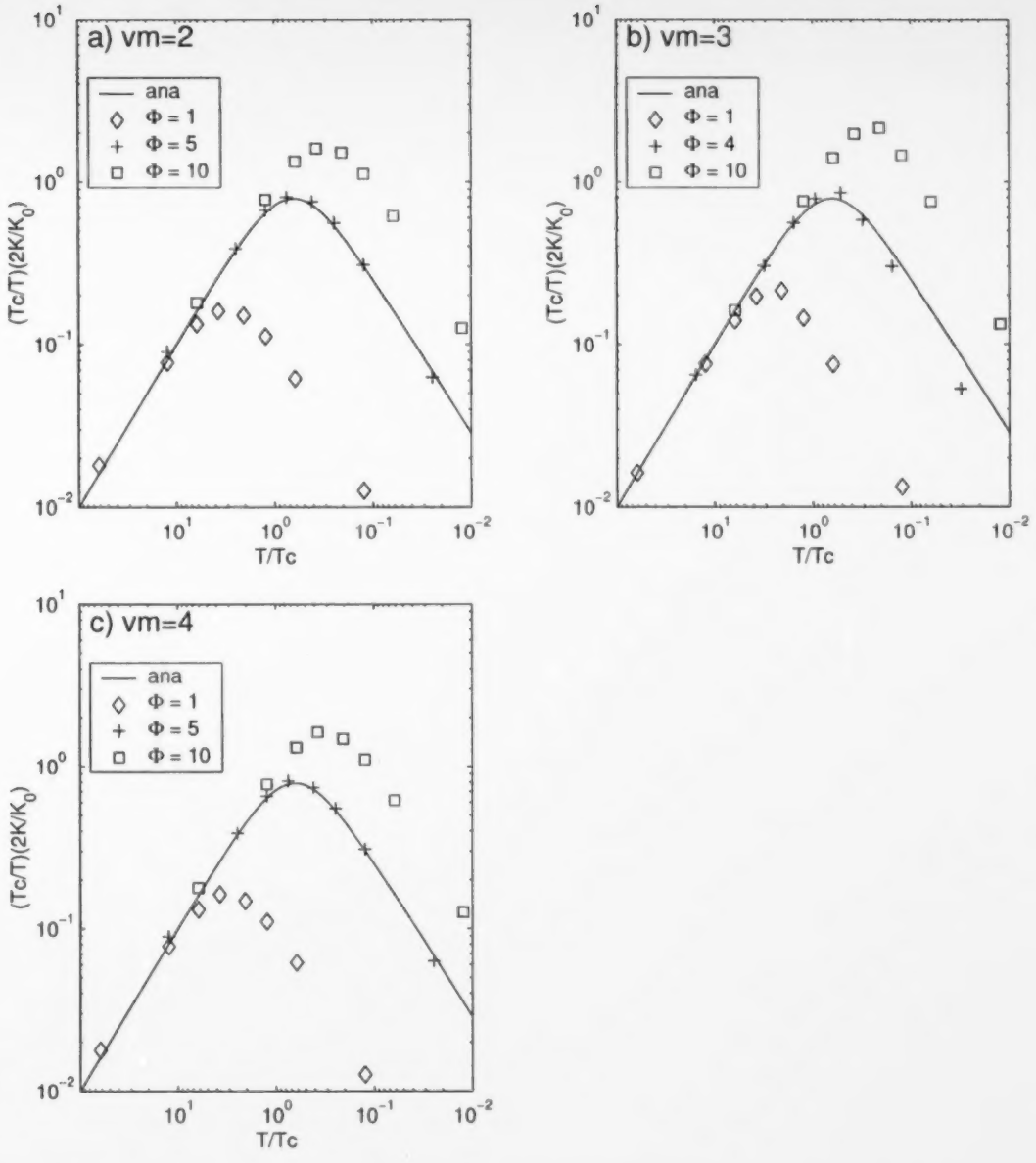

Figure 21: The diffusivity as a function of the strength of the mixing for the rotary currents case. The diffusivities from Fig. 19 have been scaled to correspond with Fig. 7.4 in Fischer et al. (1979): $(T_c/T)K/(K_0/2)$, where $K_0 = \lambda t_m$ and λ is the slope of the steady results in Figure 19. The analytical solution (37) is the solid line. The results are shown for three different time scalings of the form $t_m = T_c/\Phi$, for each of the 3 vertical shuffling methods (vm).

```
   -84.17    232.64  250 0.0035 0.1035
   236.17     81.57  250 0.0035 0.1035
    84.99   -232.42  250 0.0035 0.1035
  -235.36    -81.34  250 0.0035 0.1035
  -169.21    470.70  250 0.0035 0.1035
   471.46    168.58  250 0.0035 0.1035
   170.04   -470.48  250 0.0035 0.1035
  -462.63   -167.64  250 0.0035 0.1035
  -338.33    935.77  250 0.0035 0.1035
   942.02    342.61  250 0.0035 0.1035
   340.17   -946.60  250 0.0035 0.1035
  -933.26   -341.58  250 0.0035 0.1035
 -1016.54   2818.21  250 0.0035 0.1035
  2817.9    1016.26  250 0.0035 0.1035
  1018.96  -2828.91  250 0.0035 0.1035
 -2809.83  -1014.16  250 0.0035 0.1035
  1277.0    2714.6   250 0.0035 0.1035
  2714.6   -1277.0   250 0.0035 0.1035
 -1277.0   -2714.6   250 0.0035 0.1035
 -2714.6    1277.0   250 0.0035 0.1035
 -1694.44   4700.71  250 0.0035 0.1035
  4693.44   1690.44  250 0.0035 0.1035
  1697.10  -4700.07  250 0.0035 0.1035
 -4686.74  -1686.22  250 0.0035 0.1035
  2128.3    4524.4   250 0.0035 0.1035
 -2128.3   -4524.4   250 0.0035 0.1035
 -4524.4    2128.3   250 0.0035 0.1035
  2541.5    7056.3   250 0.0035 0.1035
  7056.3    2541.5   250 0.0035 0.1035
  2541.5   -7056.3   250 0.0035 0.1035
 -3192.4   -6786.6   250 0.0035 0.1035
 -7056.3   -2541.5   250 0.0035 0.1035
 -3388.6    9408.4   250 0.0035 0.1035
  9408.4    3388.6   250 0.0035 0.1035
 -9408.4   -3388.6   250 0.0035 0.1035
 -9048.8    4256.6   250 0.0035 0.1035
 18817.0    6777.2   250 0.0035 0.1035
-18817.0   -6777.2   250 0.0035 0.1035
1.0
data/NorthTriumph/test1out/cnstrmp.out
31 -6000 6000 31 -6000 6000 0.0035 0.1035
1.0
data/NorthTriumph/test1out/biology.out
0.1 0.5
1.0
data/NorthTriumph/test1out/biologymap.out
0.1 0.5
```

F Sample Input Time Series

The input time series files shown in this Section can be found in `data/NorthTriumph/currents/`. More information is available in Sections 5 and 6.

F.1 Friction Velocity Time Series

Below is the beginning of a friction velocity `bblt v7.0` input file (Line 8 in Section 5.2). Lines before `XXXX` are ignored. After that come two header lines, followed by year of observations, and number of columns in data file. The first column is the time in year days, the second is the total wave-current friction velocity, the third is the total current friction velocity and the third the wave-current boundary height.

```
FILE NAME: TS2eUe3_UST2L_1.dat
Generated by SEDTRANS 96 from 67m current meter
file and AE40 wave hindcast.
XXXX
2 layer friction for NT
time u*cw u*c delta_cw
1999
4
270.708 0.00843 0.00843 0.00000
270.750 0.00933 0.00933 0.00000
270.792 0.01062 0.01062 0.00000
270.833 0.00919 0.00919 0.00000
270.875 0.00709 0.00709 0.00000
270.917 0.00528 0.00528 0.00000
270.958 0.00214 0.00214 0.00000
271.000 0.00314 0.00314 0.00000
271.042 0.00252 0.00252 0.00000
271.083 0.00286 0.00286 0.00000
```

F.2 Discharge Time Series

Below is the beginning of a sample discharge time series `bblt` input file (Line 8 in Section 5.2). Lines before `XXXX` are ignored. The next line must contain the individual packet mass in grams. This is followed by an arbitrary comment line, year of observations and number of columns in the data file. The first column is the time in yeardays and the second is the total number of packets to be added during each time step. The time stamp needs not be uniform and zeros are allowed for the number of packets. If no packets are released at the start of a simulation, the code keeps skipping advection steps until packets are encountered. If this happens, no output is written and a warning is sent to the screen.

```
FILE NAME:  NT1-HIGH1Hstep_60K.o1d
mass inputs for scenario 1
time in hours (START DATE =03-Oct-99 )
total number of packets =  59935
XXXX
3536.0 packet mass (g)
time npackets mass1 mass0
1999
2
  276.7080 138
  276.7500 138
  276.7920 138
  276.8330 138
  276.8750 138
  276.9170 138
  276.9580 138
  277.0000 138
  277.0420 138
  277.0830 138
  277.1250 138
  277.1670 138
  277.2080 2
```

F.3 Velocity Time Series

Below is the beginning of a current meter `bblt` input file (Line 15 in Section 5.2). Lines before `XXXX` are ignored. After that come two header lines, followed by year of observations, and number of columns in data file. The first column is the time in yeardays, the second is the $u-$component of velocity and the third is the $v-$component. The $u-$component is east-west (positive east), and the $v-$component is north-south (positive north). It's important to insure that there are no gaps in the data and that the interval between data points is constant (and equal to Δt_V).

```
FILE NAME: TS2eUe3_67m_1.o1d
67 m depth current meter
XXXX
North Triumph
time(yd) u(m/s) v(m/s)
1999
3
270.7083 -0.09637 -0.14813
270.7500 -0.18279 -0.06971
270.7917 -0.20730 -0.08224
270.8333 -0.18582 -0.05287
270.8750 -0.14900 0.00756
270.9167 -0.10353 0.03921
270.9583 -0.03497 -0.02764
271.0000 -0.05122 -0.04085
```

```
271.0417 -0.05297 0.00053
271.0833 0.00388 0.05979
```

G Sample Auxiliary Files

The input auxiliary files shown in this Section can be found in `data/NorthTriumph/currents/`. More information is available in Sections 5 and 6.

G.1 Log-layer File

Below is the sample log-layer file (Line 13 in Section 5.2). For this case, the bottom current meter is 3 mab, so the heights in the log-layer are defined between the reference height (0.0035 m) and 3 m. They are approximately logarithmically spaced. The lines before `XXXX` are header lines. The following line is the number of vertical positions in the file followed by the positions themselves.

```
FILE NAME: hloglayer2.3m
log-layer heights for shear in bottom 3 m.
XXXX
 25
 0.0035
 0.0040
 0.005
 0.006
 0.007
 0.008
 0.01
 0.012
 0.015
 0.018
 0.02
 0.03
 0.04
 0.05
 0.06
 0.07
 0.08
 0.1
 0.2
 0.3
 0.5
 0.7
 1.0
 2.0
 3.0
```

G.2 Height File

Below is the sample currents heights file (Line 14 in Section 5.2). The lines before `XXXX` are header lines. Next comes the number of depths below the surface followed by a list of the depths of the current observations starting with the bottom current meter.

```
FILENAME: TS2eUe3.heights
North Triumph Study
distance below the surface
XXXX
8
-67
-65
-63
-61
-56
-51
-41
-31
```

H Sample Outputs

The output files shown in this Section can be found in `data/NorthTriumph/goodout/`. More information is available in Sections 3.9, 5 and 6.

H.1 Sediment Parameters File (`sedparams.out`)

Below are the first 10 lines of the sediment parameters output file generated by the North Triumph example (dots depict line continuation). The columns are: time (days), u_{*cw}, u_{*c}, δ_{cw}, 4 Rouse numbers p_1, p_{1in}, p_2 and p_{2in}, total packets N, the total number of packets that had experienced breakup at least once N_b and the settling velocity of the N_b packets. The module that generates this file is **`sedout`**.

```
0.27675E+03 .3743E-02 .3743E-02 .0000E+00 .494E+00 .247E+01 .494E+00 ...
0.27679E+03 .1076E-01 .1076E-01 .0000E+00 .172E-01 .860E+00 .172E-01
0.27683E+03 .8213E-02 .8213E-02 .0000E+00 .225E+00 .113E+01 .225E+00
0.27687E+03 .7015E-02 .7015E-02 .0000E+00 .264E+00 .132E+01 .264E+00
0.27691E+03 .6266E-02 .6266E-02 .0000E+00 .295E+00 .148E+01 .295E+00
0.27696E+03 .1209E-01 .1209E-01 .0000E+00 .153E-01 .765E+00 .153E-01
0.27700E+03 .1008E-01 .1008E-01 .0000E+00 .183E-01 .917E+00 .183E-01
0.27704E+03 .1170E-01 .1170E-01 .0000E+00 .158E-01 .791E+00 .158E-01
0.27708E+03 .8247E-02 .8247E-02 .0000E+00 .224E+00 .112E+01 .224E+00
0.27712E+03 .4231E-02 .4231E-02 .0000E+00 .437E+00 .219E+01 .437E+00 ...
```

```
...     .247E+01     138       0 .10E-02
        .860E+00     276     276 .10E-03
        .113E+01     414     414 .10E-02
        .132E+01     552     414 .10E-02
        .148E+01     690     414 .10E-02
        .765E+00     828     828 .10E-03
        .917E+00     966     966 .10E-03
        .791E+00    1104    1104 .10E-03
        .112E+01    1242    1242 .10E-02
...     .219E+01    1380    1242 .10E-02
```

H.2 Statistics File (`stats.out`)

Below are the first 10 lines of the statistics file (dots depict line continuation). The columns are time, $\overline{X}$, $\overline{Y}$, $\overline{Z}$, σ^2_{max}, σ^2_{min}, θ, $c1$, $c2$, where time is in yeardays, ($\overline{X}$, $\overline{Y}$, $\overline{Z}$) is the center of mass of the sediment in meters, σ^2_{max} and σ^2_{min} are the variances of the major and minor axes, θ is the angle that the axis of maximum variance makes with the x-axis (positive = counter clockwise), $c1$ is the depth-integrated or 2-d concentration ($\mathrm{g\,m^{-2}}$) at the center of mass, and $c2$ is the 3-d concentration ($\mathrm{g\,m^{-3}}$) at the center of mass for the user defined cylinder.

```
0.27674997E+03 0.4432E+01 -.4420E+01 0.9282E-02 0.3306E+02 0.2763E+00 ...
0.27679163E+03 0.1271E+03 -.2030E+03 0.1465E+02 0.4590E+04 0.1192E+04
0.27683330E+03 0.2680E+03 -.5996E+03 0.1296E+02 0.7240E+05 0.1552E+05
0.27687497E+03 0.3046E+03 -.7186E+03 0.9878E+01 0.2151E+06 0.6574E+05
0.27691663E+03 0.3724E+03 -.6893E+03 0.7721E+01 0.3372E+06 0.9698E+05
0.27695830E+03 0.6447E+03 -.7883E+03 0.1503E+02 0.4200E+06 0.1023E+06
0.27699997E+03 0.1029E+04 -.1074E+04 0.1508E+02 0.5108E+06 0.9492E+05
0.27704163E+03 0.1262E+04 -.1444E+04 0.1506E+02 0.7314E+06 0.9275E+05
0.27708330E+03 0.1261E+04 -.1939E+04 0.1322E+02 0.1101E+07 0.1057E+06
0.27712497E+03 0.9675E+03 -.2195E+04 0.9911E+01 0.1623E+07 0.1782E+06 ...
```

```
... -.4320E+02 0.2485E+01 0.2449E+02
    -.5840E+02 0.4934E+01 0.3602E+00
    -.3006E+02 0.4448E+01 0.3602E+00
    -.4993E+02 0.8284E+00 0.1801E+00
    -.5383E+02 0.3061E+00 0.1801E+00
    -.5325E+02 0.1621E+00 0.0000E+00
    -.5126E+02 0.6483E+00 0.0000E+00
    -.4887E+02 0.2845E+01 0.0000E+00
    -.5014E+02 0.2323E+01 0.3602E+00
... -.5756E+02 0.1189E+01 0.3602E+00
```

H.3 Concentration File (`cnstr.out`)

Below is a sample concentration time series file generated by the North Triumph example. After two comment header lines, `bblt` lists the positions of the time series locations in x, y and z.

```
Concentration
x y z number_of_positions: 38
-84.1699982  232.639999  0.0535000004
 236.169998  81.5699997  0.0535000004
 84.9899979 -232.419998  0.0535000004
-235.360001 -81.3399963  0.0535000004
-169.210007  470.700012  0.0535000004
 471.459991  168.580002  0.0535000004
 170.039993 -470.480011  0.0535000004
-462.630005 -167.639999  0.0535000004
.
.
.
```

After a blank line follow columns of numbers representing the concentrations in $\mathrm{g\,m^{-3}}$ (or $\mathrm{mg\,L^{-1}}$). The first column is time in yeardays, and all others are concentrations. There are as many columns as user-specified locations. Only the first 4 are included here.

```
0.276750E+03  0.8227E+01  0.2414E+02  0.2468E+02  0.6438E+01  ...
0.276792E+03  0.0000E+00  0.2312E-01  0.1823E+00  0.3302E-02  ...
0.276833E+03  0.0000E+00  0.0000E+00  0.5580E-01  0.3307E-01  ...
0.276875E+03  0.2516E+00  0.1107E+02  0.1699E+02  0.5032E+00  ...
0.276917E+03  0.4381E+00  0.3052E+02  0.3534E+02  0.2921E+00  ...
0.276958E+03  0.0000E+00  0.2810E-01  0.9737E-01  0.0000E+00  ...
0.277000E+03  0.0000E+00  0.1994E-02  0.9305E-02  0.0000E+00  ...
0.277042E+03  0.0000E+00  0.0000E+00  0.2032E-01  0.0000E+00  ...
```

H.4 Biological Impacts File (`biology.out`)

Below are the first 10 lines of the biological impacts file generated by the North Triumph example. The columns are as follows: station number, x, y and z coordinates of the station, percent of growth days lost and finally the total growth days lost over the whole simulation.

```
1       -84.2       232.6     0.054     14.211     5.329
2       236.2        81.6     0.054     11.962     4.486
3        85.0      -232.4     0.054     16.472     6.177
4      -235.4       -81.3     0.054     13.681     5.130
5      -169.2       470.7     0.054      2.857     1.071
6       471.5       168.6     0.054      3.285     1.232
```

7	170.0	-470.5	0.054	7.361	2.760
8	-462.6	-167.6	0.054	5.932	2.224
9	-338.3	935.8	0.054	0.638	0.239
10	942.0	342.6	0.054	2.207	0.827